5-2009

Box-Counting Dimension and Beyond

Kassie Archer
College of William and Mary

Box-Counting Dimension and Beyond

A thesis submitted in partial fulfillment of the requirement
for the degree of Bachelors of Science in **Mathematics** from
The College of William and Mary

by

Kassie Archer

Accepted for _____
(Honors, High Honors, Highest Honors)

_____
Sarah Day, Director

_____
David Lutzer

_____
R. Michael Lewis

_____
John Delos

Williamsburg, VA
March 27, 2009

Box-Counting Dimension and Beyond

Kassie Archer
Advisor: Sarah Day

March 20, 2009

Contents

Abstract

This paper explores different analytical and computational methods of computing the box-counting dimension of a fractal-like set, such as the attractor associated with a chaotic dynamical system. Because attractors cannot be described exactly, but can only be approximated by computational methods, the box-counting dimension is typically measured computationally. Using alternative measures of chaotic behavior, such as the Lyapunov exponents, it is possible to estimate the accuracy of a computational approximation. The box-counting dimension definition is extended to include subsets of regular subspaces of $\mathbb{R}^\infty$. These sets include products of Cantor sets and attractors associated with infinite dimensional dynamical systems, such as the Kot-Schaffer model. Computational approaches to computing the box-counting dimension of the Kot-Schaffer attractor are discussed and the results for this attractor are discussed.

Keywords: box-counting dimension, Lyapunov exponents, infinite dimensional dynamical systems

Acknowledgments

First and foremost, I would like to thank my honors thesis advisor, Professor Sarah Day, for all the help and guidance she's provided while working on this project over the past year. Of course, I would also like to thank Professors David Lutzer, Michael Lewis, and John Delos for serving on my defense committee along with Professor Day. I would also like to express my gratitude to the William and Mary Mathematics Department, especially the CSUMS group, who made all this research possible.

Chapter 1

Introduction

Attractors often arise in discrete dynamical systems as fixed points, periodic orbits, or 'chaotic attractors'. Chaotic attractors are typically intricate and complicated and are difficult or impossible to describe using the mathematics of calculus and geometry. In order to distinguish between different attractors, which are associated with different 'levels' of chaos, or complexity, measures can be made on the dynamics of the system or on the attractor itself. One of the more geometric-oriented measures of chaos is the *fractal dimension* of the attractor. The box-counting dimension of a set is one widely-used type of fractal dimension. In this paper, we present methods and results related to extending the idea of box-counting dimension to measure attractors associated with infinite dimensional systems, specifically an attractor associated with the Kot-Schaffer model.

Chapter 1 presents introductory material, including important definitions relating to dynamical systems, attractors, fractals, and fractal dimension. The example models used throughout the paper are also introduced here.

Chapter 2 focuses on box-counting dimension of several example sets, properties associated with box-counting dimension, and different methods of computing the box-counting dimension of a set.

Chapter 3 relates box-counting dimension to another measurement of the chaotic behavior: the Lyapunov exponents of a dynamical system. The Lyapunov exponents and the related Lyapunov dimension can be used to estimate the accuracy of the approximation of box-counting dimension and detect possibly misleading numerical results.

Chapter 4 focuses on the idea of box-counting dimension of a set which is a subset of some infinite dimensional space. This includes extending the definition of box-counting dimension to include subsets of infinite dimensional spaces and computing

the box-counting dimension of some chosen examples using this definition. Also discussed are methods associated with bounding and approximating box-counting dimension of sets in high-dimensional space (such as the projection of a set lying in an infinite dimensional space into a high, but finite, dimensional space). This is necessary because of the *curse of dimensionality*, which means higher dimensions create a problem for accurately computing box-counting dimension. This is related to the fact the the number of points required to capture a set grows dramatically (exponentially) as the dimension of the set increases. This chapter concludes by extending this idea of bounding and estimating the box-counting dimension of a set using inequalities to the infinite dimensional case.

Chapter 5 focuses on the application of what we know from previous chapters to evaluate the accuracy of the approximation of box-counting dimension of the attractor associated with the infinite-dimensional Kot-Schaffer model.

Finally, Chapter 6 concludes this paper with comments on the results presented in this paper and suggestions for possible future work related to the work presented here.

The electronic appendix for this project is located at the following website:

`http://www.math.wm.edu/~sday/archer_thesis_appendix.zip`

1.1 Attractors

Attractors arise when studying the long term behavior of dynamical systems. There are different ways to define an attractor. Intuitively, one thinks of the attractor as the set that most orbits enter 'in the limit'. The definition used here from Alligood, et al. [2] is a mathematical definition that agrees well with the intuitive definition of the attractor.

Definition 1.1.1. Given a discrete dynamical system associated with map

$$f : X \to X,$$

and some $x \in X$, the *(forward) orbit of x under f* is

$$\{x, f(x), f^2(x), \ldots, f^n(x), \ldots\}$$

where

$$f^k(x) = \underbrace{f(f(\ldots f(x)\ldots))}_{\text{evaluated } k \text{ times}}.$$

Definition 1.1.2. A point x is *periodic* when $f^k(x) = x$ for some finite positive k. When k is the minimal positive integer such that $f^k(x) = x$, then the orbit of x is then called a *k-periodic orbit*.

Definition 1.1.3. For a map f and initial $x_0 \in X$, the *forward limit set* of the orbit of x_0 under f is

$$\omega(x_0) = \{x : \text{for all } N \text{ and } \epsilon > 0 \text{ there exists } n > N \text{ such that } |f^n(x_0) - x| < \epsilon\}.$$

Basically, the forward limit set is the set that an orbit "converges to" in the limit.

Definition 1.1.4. An orbit is *asymptotically periodic* when it converges to a periodic orbit as $n \to \infty$. This means that the forward limit set of an asymptotically periodic orbit is a periodic orbit, a set of a finite number of points.

Definition 1.1.5. An orbit is said to be *chaotic* when it is bounded but not periodic or asymptotically periodic.

A system is generally considered a *chaotic system* when there exists a chaotic orbit for some $x \in X$.

Definition 1.1.6. A *chaotic set* is a forward limit set $\omega(x_0)$ where the orbit of x_0 is a chaotic orbit and $x_0 \in \omega(x_0)$.

In other words, a chaotic set is a forward limit set of a chaotic orbit which is contained in its own forward limit set.

Definition 1.1.7. For points $x_0, x_1 \in X$, x_1 is *attracted* to $\omega(x_0)$ if $\omega(x_1) \subset \omega(x_0)$. An *attractor* is a forward limit set that attracts a set of initial values with nonzero measure. For the attractor $A = \omega(x_0)$, the set of all x_1 with $\omega(x_1) \subset \omega(x_0) = A$ is called the *basin of attraction* of the attractor. A *chaotic attractor* (or *strange attractor*) is a chaotic set that is also an attractor.

The attractor is an invariant set (for $A \subset X$, $f(A) \subset A$) that some set of nonzero measure in the phase space "limits to" under iteration. Here, the *phase space* refers to the domain of the map. The *dimension of a map* is exactly the dimension of the phase space.

1.2 Models

The three example systems considered in this paper all exhibit chaotic behavior (and have chaotic attractors associated with them) at certain parameter values. These models are the Hénon Model, the LPA Model, and the Kot-Schaffer Model.

1.2.1 The Hénon Model

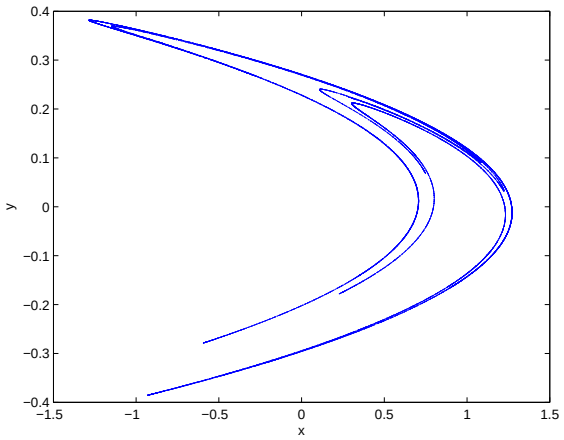

Figure 1.1: The Hénon Attractor for the parameters $a = 1.4$ and $b = 0.3$

The real Hénon family includes the 2-dimensional, discrete-time, real-valued maps governed by:

$$H : (x, y) \to (1 - ax^2 + by, x)$$

where parameters $a, b \in \mathbb{R}$. An example of a Hénon chaotic attractor for the parameters $a = 1.4$, $b = 0.3$ can be seen in Figure 1.1. These parameter values are called the canonical parameter values for Hénon [2].

This map was originally developed by M. Hénon as a simplified way of modeling the stretching and folding behavior observed in weather models. The Hénon map is one of the most-studied maps in discrete dynamics because of both its simple form and complicated behavior.

1.2.2 The LPA Model

The LPA (Larva-Pupae-Adult) model is a three-dimensional dynamical system governed by the map:

$$T(x, y, z) = (f \cdot (x + y + z) \cdot e^{-\lambda(x+y+z)}, p_1 x, p_2 y)$$

with parameters $\lambda, p_1, p_2, f \in \mathbb{R}$ [12]. For our purposes, we set the parameter values $\lambda = .1$, $p_1 = .8$, $p_2 = .6$, and consider the one-parameter family with $f \in \mathbb{R}$. Figure 1.2 shows two attractors associated with the parameter values f = 67 (left) and f = 100 (right).

The LPA model is a three-dimensional nonlinear Leslie population model. In this case, the nonlinear Leslie model is an extension of the linear Leslie model using Ricker-type nonlinearity – specifically, the fertility rates are dependent upon the size of the population. The LPA model is used to model the population of flour beetles in [12]. The nonlinearity, $(x + y + z) \cdot e^{-\lambda(x+y+z)}$, in the model accounts for cannibalism seen in populations of these flour beetles.

1.2.3 The Kot-Schaffer Model

The Kot-Schaffer Model is an infinite-dimensional model governed by the map $\Phi : L^2([-\pi, \pi]) \to L^2([-\pi, \pi])$ defined:

$$\Phi[a](y) := \frac{1}{2\pi} \int_{-\pi}^{\pi} b(x, y) g[a](x) dx,$$

where $b(x, y) = b(x - y) \in L^2([-\pi, \pi])$ and $g \in L^2([-\pi, \pi])$ [5]. Examples of 2-dimensional projections of the attractor associated with the Kot-Schaffer Model for a given set of parameter values (see Chapter 5) are shown in Figure 1.3.

The Kot-Schaffer model models the dispersion of seeds over some interval. The function b is called the *dispersal kernel* and g is the *growth function* [5].

1.3 Fractal Dimension

There are many ways to define *fractal dimension* and not all definitions are equivalent. Two of the most well-known definitions of fractal dimension are the Hausdorff dimension and the box-counting dimension. The Hausdorff dimension is widely recognized as the primary mathematical definition. It is defined for every set and has nice

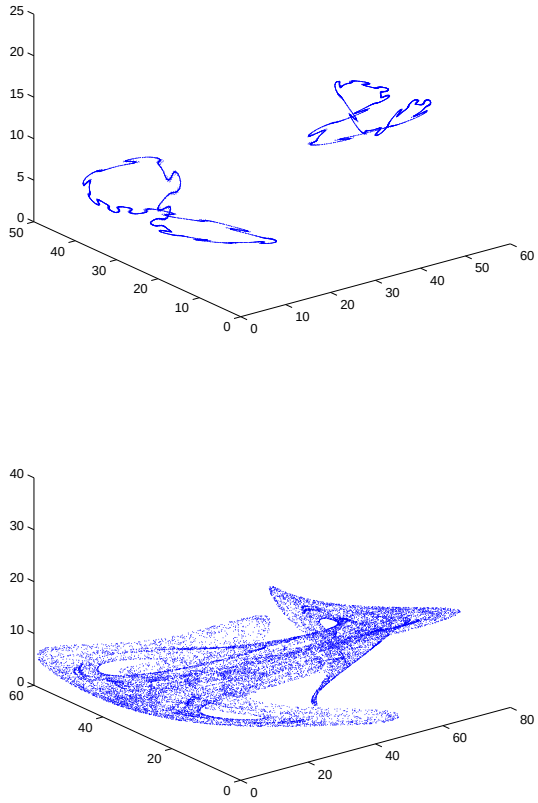

Figure 1.2: Attractors associated with the 3-dimensional Nonlinear Leslie Model at parameter values $f = 67$ (left) and $f = 100$ (right)

properties one would expect for a definition of dimension. However, the Hausdorff dimension of a set is generally very difficult to compute. Alternatively, box-counting dimension has a definition that is much more straightforward and simpler than most other definitions of fractal dimension, making computation easier.

One possible problem with box-counting dimension is that it does not exist for all sets. In these cases, it is possible to compute values called the upper and lower box-counting dimensions. When these two values are equal, we call this value the box-counting dimension. The box-counting dimension is generally assumed to exist for attractors of dynamical systems and is assumed to exist for the sets presented in this paper.

Definition 1.3.1. Let $S \subset \mathbb{R}^m$ be some nonempty bounded set. Let ϵ be the side-length, or size, of a box in $\mathbb{R}^m$ (defined to be the product of ϵ-intervals in $\mathbb{R}^m$) and $N(\epsilon)$ be the number of boxes of size ϵ needed to cover the set S.

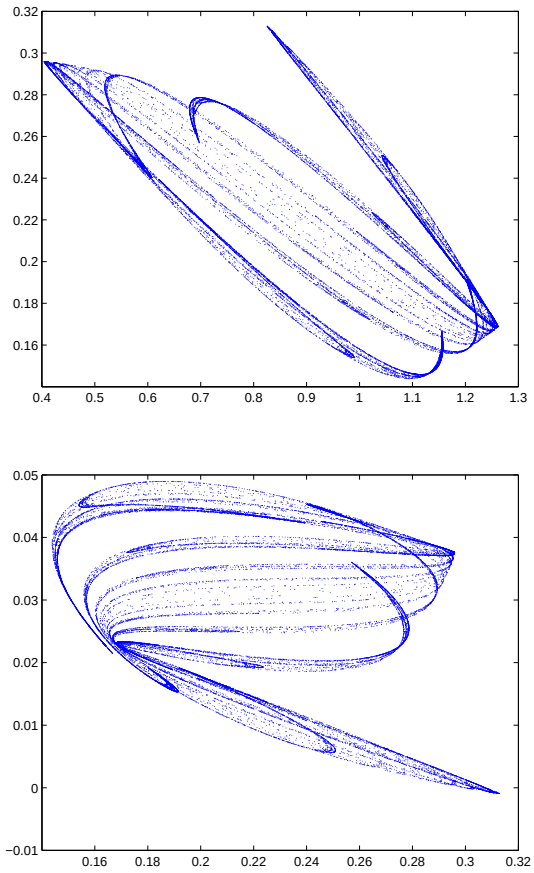

Figure 1.3: Two different 2-dimensional projections of the Kot-Schaffer attractor – these projections suggest that the attractor is a fractal-like structure and that the system exhibits chaotic behavior.

The *upper box-counting dimension* of a set S is defined as:

$$\dim_{UB}(S) = \limsup_{\epsilon \to 0} \frac{\ln(N(\epsilon))}{\ln(1/\epsilon)}.$$

The *lower box-counting dimension* of a set S is defined as:

$$\dim_{LB}(S) = \liminf_{\epsilon \to 0} \frac{\ln(N(\epsilon))}{\ln(1/\epsilon)}.$$

The *box-counting dimension* of set S is defined when

$$\dim_{LB}(S) = \dim_{UB}(S)$$

and is equal to

$$\dim_B(S) = \lim_{\epsilon \to 0} \frac{\ln(N(\epsilon))}{\ln(1/\epsilon)}.$$

Box-counting dimension can be thought of as a simplification of Hausdorff dimension. When computing Hausdorff dimension, it is necessary to choose a 'proper radius' for each box in a box-covering of the set. For box-counting dimension, one considers only ϵ-boxes of the same radius. The Hausdorff dimension and box-counting dimension are sometimes equal – for example, when we have a regular Cantor set. One example of when equality does not hold is the set $\mathbb{Q} \cap [0, 1]$. The Hausdorff dimension of this set is $\dim_H(\mathbb{Q} \cap [0, 1]) = 0$ while the box-counting dimension is $\dim_B(\mathbb{Q} \cap [0, 1]) = 1$. Generally, the following inequality holds:

$$\dim_T(S) \leq \dim_H(S) \leq \dim_B(S)$$

where $\dim_H(S)$ is the Hausdorff dimension of a set S and $\dim_T(S)$ is the topological dimension of a set S [7].

By definition, we only consider the box-counting dimension of nonempty bounded sets. The box-counting dimension of an interval, finite product of intervals, or some manifold of $\mathbb{R}^n$ corresponds to its integer topological dimension. However, there are sets for which the box-counting dimension is strictly greater than the topological dimension, some of which are fractals. This property alone is neither a sufficient nor necessary condition for a set to be defined as a fractal: some fractals will not have this property while some sets with this property are not necessarily fractals.

A *fractal* is not well defined in mathematics, but rather can be described as exhibiting properties including:

- a recursive definition or *self-similarity* (A is *self-similar* if $\lambda * B = A$ for some scalar λ and some proper subset $B \subset A$. If this property holds 'approximately', we still say the set is self-similar.)
- fine, irregular structure which cannot be described using calculus or Euclidean geometry
- complexity on arbitrarily small scales
- fractal dimension, such as the box-counting dimension, strictly greater than topological dimension [6].

We call a set *fractal-like* when it satisfies some subset of these properties. Note that self-similarity alone is not sufficient to be considered fractal-like – an interval, for example, is self-similar, but is not considered fractal-like.

In the study of dynamical systems, chaotic attractors are known to have some fractal-like structure. Computing the fractal dimension of these attractors gives us a way of measuring and comparing attractors associated with different parameters. In general, computing fractal dimension gives a way of telling how much the set "fills up space" and gives a scaling factor of the set, which reflects the self-similarity of a fractal-like set. There is also often a physical interpretation of strange attractors and fractal-like sets that may occur in the study of a dynamical system from physics or biology. Since we cannot describe fractal-like sets using typical geometric methods and in general cannot describe them at all, fractal dimension gives us a way of measuring, understanding and comparing the geometry of the sets.

Chapter 2

Box-Counting Dimension

Since the box-counting dimension of a set is not dependent on any dynamics-related information, but rather the geometry of the set, it is possible to measure the box-counting dimension of arbitrary non-empty, bounded sets that are not necessarily attractors. In Section 2.1, the box-counting dimension of several examples of non-attractor sets are measured. Following that are the methods for computing box-counting dimension and the approximations we get for attractors associated with the Hénon and LPA Models.

2.1 Basic Examples

Using the definition of box-counting dimension, if the limit exists for all ϵ going to zero, it is sufficient to use a subsequence ϵ_n of ϵ such that $\epsilon_n \to 0$ as $n \to \infty$. Also, boxes do not have to be in a fixed grid. It is allowed and sometimes preferred to move around boxes to "improve efficiency", though the if box-counting dimension exists, then the limit converges for both the fixed grid and the 'efficient' grid. However, we do use a fixed grid when finding the box-counting dimension of a set computationally.

The 'ϵ-boxes' in the definition of box-counting dimension do not necessarily have to be m-dimensional cubes. They may be triangles (used for measuring the box-counting dimension of a set called the Sierpinski gasket), rectangles, or other shapes. The only requirement is that the shape of the box not change and the size of the boxes goes to zero as $\epsilon \to 0$ [2].

2.1.1 Interval, square, & cube

The interval, square, and cube are all examples of sets with the property that the box-counting dimension agrees with the topological dimension since for these sets there is no fractal-like geometry associated with these sets.

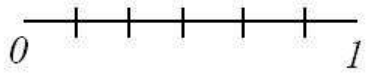

Figure 2.1: Unit Interval

Example 2.1.1. If we want to find the box-counting dimension of the unit interval, we can use the method of choosing some subsequence ϵ_n going to zero to compute the box-counting dimension from the definition.

Choose the subsequence $\epsilon_n = \frac{1}{2^n}$. Since we are dealing with the unit interval, we know that for a box of size $1/k$, we need k boxes to cover the set. So for a box of size ϵ_n, we need 2^n boxes to cover the set. So we can compute the dimension to be:

$$\dim_B(I) = \lim_{n\to\infty} \frac{\ln(N_{\epsilon_n}(I))}{\ln(1/\epsilon_n)} = \lim_{n\to\infty} \frac{\ln(2^n)}{\ln(2^n)} = \lim_{n\to\infty} \frac{n \cdot \ln(2)}{n \cdot \ln(2)} = \frac{\ln(2)}{\ln(2)} = 1.$$

So, for the unit interval, or any interval (see Theorem 2.2.2), the box-counting dimension is equal to the topological dimension.

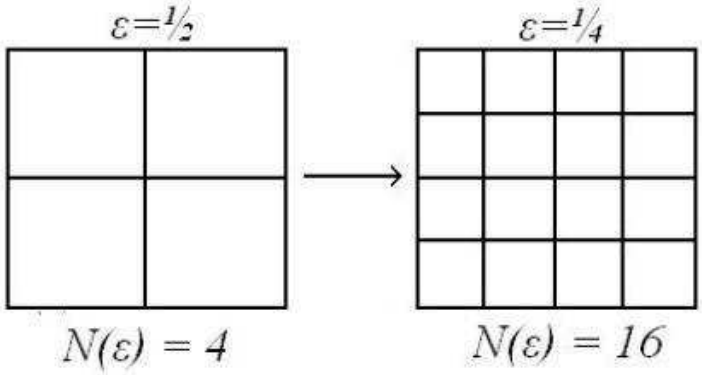

Figure 2.2: Unit Square

Example 2.1.2. If we do the same thing for the unit square using the same ϵ_n subsequence, we expect to get a dimension of 2. Each time we halve our box size, we need $4 = 2^2$ times as many boxes to cover the set (see Figure 2.2).

Then, we know for our subsequence $\epsilon_n = \frac{1}{2^n}$, we have $N_\epsilon(I \times I) = 4^n = 2^{2n}$. Then we compute the box-dimension of the unit square to be:

$$\dim_B(I \times I) = \lim_{n\to\infty} \frac{\ln(N_{\epsilon_n}(I^2))}{\ln(1/\epsilon_n)} = \lim_{n\to\infty} \frac{\ln(2^{2n})}{\ln(2^n)} = \lim_{n\to\infty} \frac{2n \cdot \ln(2)}{n \cdot \ln(2)} = \frac{2 \cdot \ln(2)}{\ln(2)} = 2.$$

Example 2.1.3. The same holds for the unit cube. Since each time we halve the box size, we need $8 = 2^3$ times as many boxes, so we will get a box-counting dimension:

$$\dim_B(I \times I \times I) = \lim_{n\to\infty} \frac{\ln(N_{\epsilon_n}(I^3))}{\ln(1/\epsilon_n)} = \lim_{n\to\infty} \frac{\ln(2^{3n})}{\ln(2^n)} = \lim_{n\to\infty} \frac{3n \cdot \ln(2)}{n \cdot \ln(2)} = \frac{3 \cdot \ln(2)}{\ln(2)} = 3.$$

By the same ideas, the box-counting dimension of any m-dimensional cube is $\dim_B(I^m) = m$. Of course, the box-counting dimension of a point or finite collection of points is $dim_B(\cdot) = 0$.

2.1.2 Cantor sets

One of the most basic and important fractals is the middle-thirds Cantor set. The middle-thirds Cantor set is a special case of the middle $1/m$ Cantor set, which has a recursive definition:

Definition 2.1.4. Let $m > 1$. Let I_0 be the unit interval. Given I_{n-1}, let I_n be the set of intervals resulting from removing the (open set) middle $1/m$ of all intervals in the set I_{n-1}. Let $l_{int}(I_n)$ be the length of an interval in the set I_n. Then the open middle portion removed from the an interval in the set I_n will be $\frac{l_{int}(I_n)}{m}$. For example, I_1 will be the set constructed by removing the middle $1/m$ of the unit interval, $[0, 1]$, resulting in the set $[0, \frac{m-1}{2m}] \bigcup [\frac{m+1}{2m}, 1]$. Then the *middle* $1/m$ *Cantor set* is

$$C = \bigcap_{j=0}^{\infty} I_j$$

thus recursively removing the middle $1/m$ of all intervals starting with the unit interval.

The *middle-thirds Cantor set* is exactly the middle $1/m$ Cantor set for $m = 3$.

Cantor sets are totally disconnected, compact metric spaces with topological dimension zero and a positive box-counting dimension. The middle-thirds Cantor set is important in the study of fractal dimension because of its nice structure and def-

inition. It is an example of a fractal whose Hausdorff dimension is equal to its box-counting dimension, both of which may be determined analytically. We compute the box-counting dimension of the middle-thirds Cantor set as an example and give the box-counting dimension (dependent on m) of a general $1/m$-Cantor set.

Example 2.1.5. The box-counting dimension is known to exist for Cantor sets [2]. To compute the box-counting dimension of a middle-thirds Cantor set, we exploit the recursive definition to make computations easier. Choose $\epsilon_n = l_{int}(I_n)$. In the middle-thirds case, the length of an interval in I_n is $l_{int}(I_n) = \frac{1}{3^n}$. For each iteration, the number of intervals doubles, and so at the n^{th} iteration, we need 2^n boxes of size ϵ_n to cover the set. Then:

$$\dim_B(C_3) = \lim_{n\to\infty} \frac{\ln(N(\epsilon_n))}{\ln(1/\epsilon_n)} = \lim_{n\to\infty} \frac{\ln(2^n)}{\ln(3^n)} = \lim_{n\to\infty} \frac{n\cdot\ln(2)}{n\cdot\ln(3)} = \frac{\ln(2)}{\ln(3)}.$$

In the general case of finding the box-counting dimension of the middle $1/m$ Cantor set, C_m, we again choose ϵ_n to be the length of an interval at the nth iteration and let $N(\epsilon_n) = 2^n$ since the number of intervals always doubles for each iteration. The length of one interval in I_n is

$$\epsilon_n = l_{int}(I_n) = \left(\frac{m-1}{2m}\right)^n.$$

So the box-counting dimension of a middle $1/m$ Cantor set C is

$$\dim_B(C_m) = \lim_{n\to\infty} \frac{\ln(2^n)}{\ln(\frac{1}{(\frac{m-1}{2m})^n})} = \frac{\ln(2)}{\ln(\frac{2m}{m-1})}. \tag{2.1}$$

The following Theorem follows from this property.

Theorem 2.1.6. *For any $d \in (0,1)$, there is a middle $1/m$ Cantor set with dimension d.*

Proof. Choose m to be:

$$m = \frac{2^{1/d}}{2^{1/d} - 2}.$$

Then, by Equation 2.1, $\dim_B(C_m) = d$. □

Since m can be any real number greater than 1, we can find a Cantor set of any dimension between 0 and 1. This fact will be important later for an example in Section 4.1.1.

Definition 2.1.7. A *modified Cantor set* $\hat{C}$ is defined here to be a set constructed from removing relatively bigger open-middles from intervals at each iteration. Let

$a = \{a_i\}_{i=1}^{\infty}$ be some decreasing sequence which converges to zero so that $a_1 < 1$. Let I_0 be the unit interval. Let I_n be the set resulting from removing the (open) middle of all intervals in the set I_{n-1} so that $l_{int}(I_n) = a_n * l_{int}(I_{n-1})$ where $l_{int}(I_i)$ is the length of an interval in I_i. Then the modified Cantor set is

$$C = \bigcap_{j=0}^{\infty} I_j$$

thus recursively removing relatively larger open-middles of all intervals starting with the unit interval.

Example 2.1.8. Here we define the example modified Cantor Set so that at each iteration i, the length of the interval left is $1/4^i$ the length of the previous interval. So, after the first iteration, two intervals of length $1/4$ are remaining. After two iterations, four intervals of $1/16$th the length of the previous interval (length $1/64$) are remaining. After n iterations, 2^n intervals of length $l_{int}(I_n) = 2^{-(n^2+n)}$ are remaining. (This results from removing the middle $(\frac{1}{2^{((n-1)^2+(n-1))}} - \frac{2}{2^{(n^2+n)}})$th from all intervals at the nth iteration.)

Let $\epsilon_n = l_{int}(I_n) = 2^{-(n^2+n)}$. Then we have:

$$\dim_B(\hat{C}) = \lim_{n\to\infty} \frac{\ln(N(\epsilon_n))}{\ln(1/\epsilon_n)} = \lim_{n\to\infty} \frac{\ln(2^n)}{\ln(2^{n^2+n})} = \lim_{n\to\infty} \frac{n}{n^2+n} = 0.$$

Though our example of a modified Cantor set has box-counting dimension 0, we still call it a fractal-like set because of its recursive definition and complexity on arbitrarily small scales. This set will be used to construct an interesting example of an infinite dimensional fractal-like set in Example 4.1.1.

2.2 Some Properties of Box-counting Dimension

Theorem 2.2.1. *For a subset $B \subset S$,*

$$\dim_B(B) \leq \dim_B(S).$$

Proof. For any ϵ, $N_\epsilon(S)$ ϵ-boxes cover the set S Since for any $b \in B$, $b \in S$ also, then the covering of B is contained in the covering of S, so $N_\epsilon(B) \leq N_\epsilon(S)$ for the same ϵ. □

This theorem shows the invariance of box-counting dimension under scaling.

Theorem 2.2.2. *Box-counting dimension is invariant under scaling.*

Proof. Assume our set S is scaled by some constant c. We can call this new set S_c. Then we can let our ϵ_{S_c} be $c \cdot \epsilon_S$ so that the number of boxes we need to cover the set is the same. The box dimension of the new set is:

$$\dim_B(S_c) = \lim_{\epsilon_{S_c}\to 0}\frac{\ln(N_{\epsilon_{S_c}}(S_c)))}{\ln(1/\epsilon_{S_c})} = \lim_{\epsilon_S\to 0}\frac{\ln(N_{\epsilon_S}(S))}{\ln(\frac{1}{c\cdot\epsilon_S})} = \lim_{\epsilon_S\to 0}\frac{\ln(N_{\epsilon_S}(S))}{\ln(1/c)+\ln(1/\epsilon_S)}.$$

Since $\ln(1/c)$ is a constant, in the limit the box-counting dimensions of the two sets are equal. □

Theorem 2.2.3 will be important later when measuring the box-counting dimension of infinite products of Cantor sets.

Theorem 2.2.3. *If $C = \prod_{i=1}^{n} C_i$, with C_i a middle $1/m_i$ Cantor set for all $i = 1, 2, ..., n$, then*

$$\dim_B(C) = \sum_{i=1}^{n} \dim_B(C_i).$$

Proof. Since we are using uniform Cantor sets, the box-counting dimension exists and is finite for all C_i. Then we can let ϵ be the same for all sets C_i. By definition of box-counting dimension,

$$\begin{aligned}
\sum_{i=1}^{n} \dim_B(C_i) &= \sum_{i=1}^{n} \lim_{\epsilon\to 0} \frac{\ln(N_\epsilon(C_i))}{\ln(1/\epsilon)} \\
&= \lim_{\epsilon\to 0} \sum_{i=1}^{n} \frac{\ln(N_\epsilon(C_i))}{\ln(1/\epsilon)} \\
&= \lim_{\epsilon\to 0} \frac{\sum_{i=1}^{n} \ln(N_\epsilon(C_i))}{\ln(1/\epsilon)} \\
&= \lim_{\epsilon\to 0} \frac{\ln(\prod_{i=1}^{n} N_\epsilon(C_i))}{\ln(1/\epsilon)}.
\end{aligned}$$

Since C is the Cartesian product of nonempty Cantor Sets $C_1, C_2, ..., C_n$, if $a_i \in C_i$ then $(a_1, a_2, ..., a_n) \in C$. If a 1-dimensional ϵ-box is needed to cover a_i for each i and all ϵs are equal, then an n-dimensional ϵ-box is needed to cover $(a_1, a_2, ..., a_n) \in C$. So $N_\epsilon(C) = \prod_{i=1}^{n} N_\epsilon(C_i)$. Then the box-counting dimension of C is:

$$\dim_B(C) = \lim_{\epsilon\to 0} \frac{\ln(\prod_{i=1}^{n} N_\epsilon(C_i))}{\ln(1/\epsilon)}.$$

Equality holds in the case of Cantor sets, but in the general case for sets A and B we have:

$$\dim_B(A \times B) \leq \dim_B(A) + \dim_B(B).$$

This is apparent since any point $(a, b) \in A \times B$ with $a \in A$ and $b \in B$ will at least be covered by the box $I \times J$ where I is the box in A that covers a and J is the box in B that covers b [7].

By a similar argument, we can show that the box-counting dimension of a finite product of our example of a modified Cantor set:

$$\hat{C}_P = \prod_{j=1}^{n} \hat{C}_j, \quad \hat{C}_j = \hat{C}, \ \forall j$$

is $\dim_B(\hat{C}_P = 0)$.

2.3 Computational Methods

Since chaotic attractors typically exhibit geometry too complicated to describe analytically and box-counting dimension is a measure on the geometry of a set, the box-counting dimension of a chaotic attractor is measured computationally. When dealing with an attractor or some other set that can only be approximated computationally, it is convenient to have an efficient method to compute the box-counting dimension of this set.

For all methods of computation of the box-counting dimension we consider, the map is iterated an appropriate number of times (called K_1 times) starting at some initial point and the first K_0 iterates are thrown out, so that the $(K_0 + 1)$st through the K_1st points are considered an approximation of the attractor:

```
A(:,1) = (x_0,y_0) % x_0, y_0 are initial values
for j = 2:K_1
A(:,j) = H(A(:,j-1));
end
A(:,K_0:K_1) approximates attractor.
```

The initial point can be chosen from almost anywhere in the basin of attraction of the attractor, a set of nonzero measure whose forward limit set is the attractor.

For our methods, a program called GAIO (Global Analysis of Invariant Objects) is used to create a grid in the phase space in which the attractor lies [9]. GAIO

uses a tree-structure to "hold" m-dimensional boxes, where m is the dimension of the phase space. The root of the tree is the initial box, some single box that covers the entire attractor. This initial box is subdivided equally in the coordinate directions. The *depth* of the tree refers to the number of subdivisions that have been done to the initial box to get the grid. These boxes form a grid covering the attractor. It is possible to "throw out" certain boxes or to "insert" boxes into the tree. For the following methods, the box-covering of the attractor is obtained by inserting boxes into the tree at a certain depth, which corresponds to some ϵ value, $\epsilon = \frac{\epsilon_0}{(d/m)}$, where ϵ_0 is the size of the initial box and the depth, d, is divided by the dimension of the phase space, m, since the boxes are only subdivided in one coordinate direction as depth is incremented by one. Naturally, only depths of the form $d = k \cdot m$ with $k \in \mathbb{N}$ are considered when computing box-counting dimension so that these boxes will have the same shape (half the ϵ-size in each coordinate direction). If the original box is square, boxes at a depth of the form $d = k \cdot m$ with $k \in \mathbb{N}$ will also be square.

The most direct method of computing box-counting dimension is called the *subdivision method*. Here, some depth, d, (and corresponding ϵ value) is chosen, preferably a high depth (and corresponding small ϵ value). Then the box-counting dimension of a set A is approximated by: $\frac{\log(N(\epsilon_d))}{\log(1/\epsilon_d)}$, where ϵ_d corresponds to the depth d. This approximation is often not very accurate, even when assuming enough iteration points are taken. In Section 2.2.2, it is shown that box-counting dimension is invariant under scaling, but this approximation of box-counting dimension can be very skewed if the initial box size is too large or too small. Another problem is that this approximation converges slowly as ϵ decreases.

A better method for computing box-counting dimension is the *slope method*. This method involves takings several ϵ values into consideration and plotting $\log(1/\epsilon_d)$ versus $\log(N(\epsilon_d))$ for some values $d = d_1, d_2, \ldots, d_p$. The slope of this line approximates the limit of the ratio of $\log(N(\epsilon_d))$ to $\log(1/\epsilon_d)$ as $\epsilon \to 0$, the definition of box-counting dimension [10].

The method used throughout this paper is similar to the slope method. It was developed by Siegmund and Taraba [11], and has been shown to converge faster than the subdivision method as ϵ decreases (and the depth of the tree in GAIO increases). It is specifically tailored for use with GAIO. For this method, two values of depths d_1 and d_2 are considered, so that the ϵ value for the second depth is half that for the first depth ($\epsilon_{d_1} = 2 \cdot \epsilon_{d_2}$). Then use the equation:

$$\dim_B(S) = \frac{\log(N(\epsilon_{d_1})) - \log(N(\epsilon_{d_2}))}{\log(2)}$$

to approximate box-counting dimension of the set S. This is exactly the slope method with two points instead of several. Note that this value is not skewed by the size of the initial box since we only assume that $\epsilon_{d_1} = 2 \cdot \epsilon_{d_2}$. For this reason, we consider depth instead of ϵ to be the computational parameter we care about.

So to compute the box-counting dimension of an attractor, the following algorithm is used:

```
A(:,K_0,K_1) is the approximation for the attractor
for j = K_0:K_1
  tree.insert(A(:,j), d_2)  % inserts the box containing the point A(:,j)
                            % at depth d_2 (because of the tree stucture in
                            % GAIO, the box containing A(:,j) is automatically
                            % inserted at depth d_1 also)
end
N_1 = tree.count(d_1)       % number of boxes in covering at depth d_1
N_2 = tree.count(d_2)       % number of boxes in covering at depth d_2
dim_B = (log(N_1) - log(N_2))/log(2);
```

2.4 Computational Parameters

Two important computational parameters to take into consideration when computing box-counting dimension are the iteration number, K_1, and the depth, d (or the ϵ value). It is important to strike a balance between the ϵ value and K_1, the number of iterates. Ideally, one may want to let ϵ be as small as possible and the iteration number K_1 be as large as possible, but this is unrealistic because of high computational cost.

Here, we observe the effects of changing these values on the box-counting dimension approximation obtained for the Hénon attractor associated with parameters a = 1.4 and b = 0.3 (see Figure 1.1). The 'true' value of the box-counting dimension of this set should be close to 1.26.

2.4.1 Changing ϵ

Given an attractor A and a fixed value for K_1 (the number of iteration points), as ϵ gets very small, the attractor starts to look like a finite set of points instead of

an approximation for the attractor. Consider the ratio

$$\frac{\ln(N(\epsilon))}{\ln(1/\epsilon)}.$$

Since there are only a finite number, K_1 of points where boxes may be inserted, as $\epsilon \to 0$, $N(\epsilon)$ has a maximum at K_1, while $1/\epsilon \to \infty$. Therefore, for ϵ values too small for the given K_1, the box-counting dimension falls to zero.

If one uses an ϵ that is too small, the result computed may be an artificial maximum for the box-counting dimension instead of the true value of box-counting dimension. This type of error is more prevalent when using the subdivision method. In this case, for a given K_1 and ϵ, the maximal value one can compute will be $D_c = \frac{\ln(K_1)}{\ln(1/\epsilon)}$. If this value is less than the box-counting dimension of the 'true' set, then this value, D_c, will be misleading (lower than the true value).

Another problem with using ϵ values that are too small is that the numerical error from computation may be on the scale of ϵ, so that the attractor looks 'fatter' than it actually is. The important thing is to use an epsilon value that is small enough to pick up on the fractal-like structure of the set, but not so small that an excess of numerical errors gives meaningless results.

2.4.2 Changing K_1

In order to get a good estimation of the box-counting dimension, one should use a sufficient number of iteration points to approximate the attractor given some ϵ grid. For some fixed ϵ, if the value of K_1 is taken to be too small, then boxes in the 'true covering' of the attractor will be missed. The smaller the ϵ value, the larger K_1, the number of iterations, should be.

Sample Result 2.4.1. Figure 2.3 illustrates the fact that smaller ϵ values (associated with greater depth values in GAIO) need more iteration points to find the "true" ϵ-box covering of the attractor. Convergence to some approximation of box-counting dimension happens for a much smaller value of K_1 for the larger ϵ-value (depth = 6) than the smaller ϵ-value, 1/8th the size of the larger value (depth = 12).

A good way to ensure that enough iterations have been taken is by applying an adaptive algorithm that iterates an extra N number of points, for some appropriate (large) value of N, checking to see if boxes are added. If no boxes are added to the GAIO tree after iterating these extra times, then we can assume that we have a sufficient number iterations.

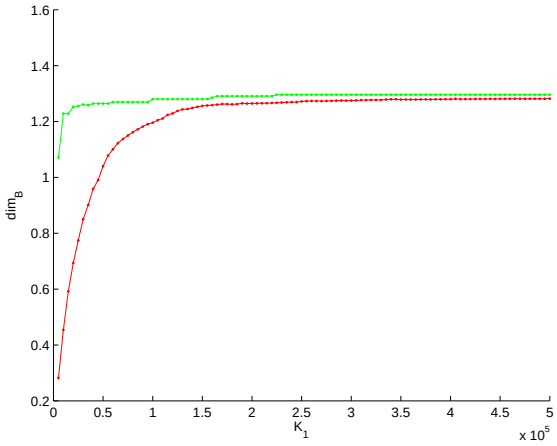

Figure 2.3: Values for the approximate box-counting dimension of the Hénon attractors (for parameters $a = 1.4$ and $b = 0.3$) at depth = 6 (green) and depth = 12 (red) as K_1 increases

Numerical results have suggested that for objects with lower box-counting dimension, the number of iterations needed is much smaller even if the object lies in a high dimensional phase space. This makes sense and is illustrated by the example of the 0-dimensional fixed point attractor. Much fewer iteration points are needed to approximate this attractor than one of a positive box-counting dimension regardless of the dimension of the phase space.

2.4.3 Using the zeroth Betti number

A useful way of checking if enough iteration points have been used is by computing the *zeroth Betti number* [8] , or the number of connected components, of the box-covering of the attractor. We can do this using a program called CHomP [1], which gives the Betti numbers associated with some set of boxes in GAIO. After inserting ϵ-boxes for K_1 iterations of some map using GAIO, we run CHomP to compute the number of connected components of this box-covering. If ϵ is too small for our given K_1, we will get a large zeroth Betti number. If we know (or believe) beforehand that our attractor should only have one connected component, this method is a good way to check if we have used enough iteration points for our given ϵ value.

This method can be very useful since there is no way to know if the K_1 used is large enough just from computing the box-counting dimension once. If the box-covering is connected, it is an indication that the covering is at least a good approximation for the true box-covering.

2.5 Computational Examples

Sample Result 2.5.1. Figure 2.4 shows the estimated box-counting dimension of the Hénon attractors for the parameter values $b = 0.3$ and $a \in [1, 1.4]$.

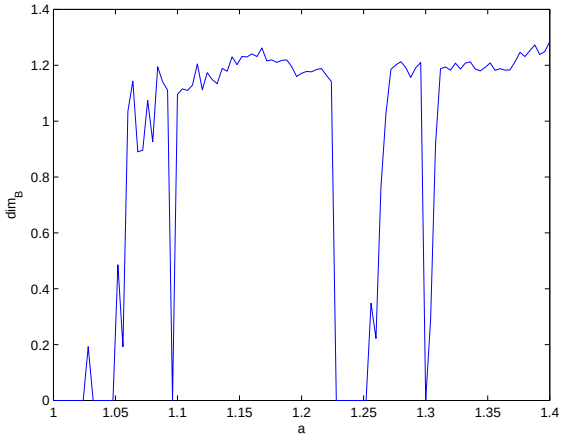

Figure 2.4: Approximate box-counting dimension of the Hénon attractors for parameter $b = 0.3$ and $a \in [1, 1.4]$

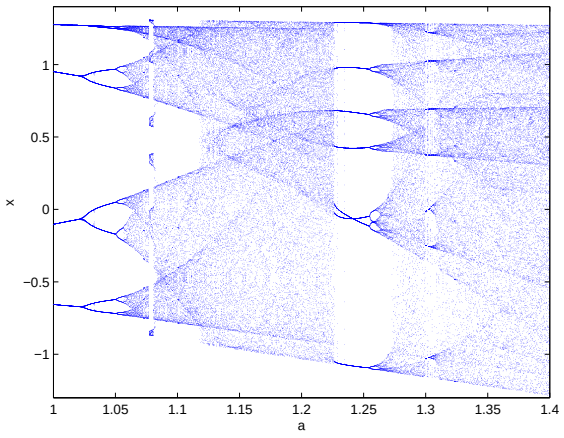

Figure 2.5: Bifurcation diagram for the Hénon model for parameter $b = 0.3$ and $a \in [1, 1.4]$

Figure 2.5 is the bifurcation diagram associated with the Hénon models for these same parameter values. The bifurcation diagram shows the x-values of the attractors as a is varied. It allows one to "see" the attractor as the parameter a changes.

We can see that for the most part the values computed for the box-counting dimension of the attractor agrees with what one should expect from the bifurcation

diagram. Where the bifurcation diagram indicates a periodic attractor, the box-counting dimension is usually zero. (For values where the box-counting dimension of a periodic attractor is not zero, see Section 3.1.2).

Sample Result 2.5.2. Recall from Section 1.2.2 that the parameters we use for the LPA model are $\lambda = .1$, $p_1 = .8$, $p_2 = .6$, with f varying. Consider the models where $f \in [50, 100]$. Figure 2.6 shows the graph of the approximate box-counting dimension of these models with computational parameters, $K_1 = 10^5$ and depth $= 18 = 6 \cdot 3$. The accuracy of these measurements is estimated in Section 3.2.2.

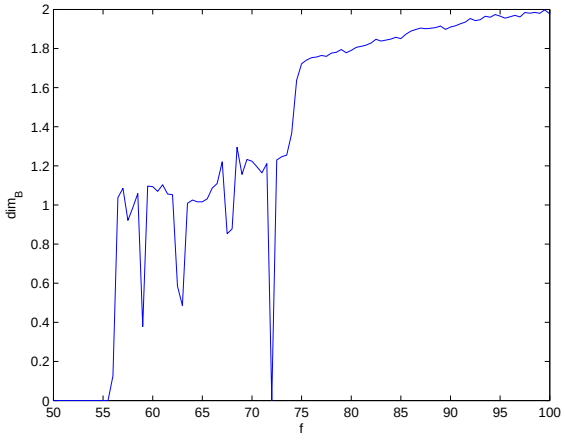

Figure 2.6: Box-counting dimension for LPA attractors associated with parameter $f \in [50, 100]$

Chapter 3

Lyapunov Exponents & Dimension

Lyapunov exponents and dimension are introduced in this chapter as a way of estimating the accuracy of our measurement of box-counting dimension. Both the Lyapunov exponents and the Lyapunov dimension can allow us to comment on the accuracy (and reasons for inaccuracy in some cases) of our approximations.

3.1 Lyapunov Exponents

The Lyapunov exponents associated with a system provide an alternative way of "measuring chaos" associated with the system. The Lyapunov exponents are not dependent on the geometry of the attractor, but rather on the map associated with the system. They give an idea about the expansion and contraction of the map at a point. A positive Lyapunov exponent is generally associated with chaotic behavior while a system with all negative exponents is associated with periodic or asymptotically periodic behvior.

Definition 3.1.1. Lyapunov exponents measure the rates of separation in m orthogonal directions (where m is the dimension of the map) upon iteration and computed from the map associated with the system. For a smooth map $f : \mathbb{R}^m \to \mathbb{R}^m$, let $J_n(x)$ be the Jacobian (matrix of partial derivatives) of the nth iteration of the map evaluated at some point $x \in \mathbb{R}^m$. When $J_n(x)$ is applied to the unit sphere, we let r_k^n be the kth longest orthogonal axis of the resulting ellipse. The set $\{r_k^n\}$ captures the expanding and contracting behavior near the orbit of x. Then the *kth Lyapunov number* at x is defined to be:

$$L_k(x) = \lim_{n\to\infty} (r_k^n)^{1/n}.$$

Then, the *kth Lyapunov exponent* at x is defined to be:

$$\lambda_k(x) = \ln(L_k(x)).$$

It follows from this definition that $\lambda_1 \geq \lambda_2 \geq \cdots \geq \lambda_m$. The largest Lyapunov exponent, λ_1, is sometimes referred to as the *maximal Lyapunov exponent*. Because of a property called *ergodicity*, almost all points in a set of nonzero measure (the basin of attraction of the attractor associated with the system) have the same Lyapunov exponents [10]. For this reason, we can refer to the Lyapunov exponents of a system, even though the Lyapunov exponents are only defined for a point [2].

Chaotic orbits exhibit sensitive dependence on initial conditions. Lyapunov exponents quantify how fast two arbitrarily close points move apart from or toward each other per iteration on average. A bounded orbit is defined as chaotic when its maximal Lyapunov exponent is positive, which means there is expansion (stretching) in at least one direction.

3.1.1 Computing the Lyapunov exponent

For computing Lyapunov exponents, we start with an arbitrary orthonormal basis $\{w_i\}$, compute a new basis $\{z_i = Df(x)w_i\}$ for almost any initial point x, then use Grahm-Schmidt orthogonalization on $\{z_i\}$ to get an orthogonal basis, $\{y_i\}$. Then set the new $w_i = y_i/||y_i||$ to obtain a new orthonormal basis $\{w_i\}$. We continue this process for N iterations for some large N, each time normalizing. Then the kth largest Lyapunov exponent will be approximated by $\frac{\sum_{j=1}^{N} \log(||y_k^{(j)}||)}{N}$ where $y_k^{(j)}$ is the jth orthogonal basis computed. Given H (the first K_1 iterations of an m-dimensional map), $\{w_j\}$ (the orthonormal basis), and x_0 (an initial point), this is demonstrated:

```
for k = 1:K_1
  J = Jacobian(H(:,k));
  for i = 1:m
  z(i) = J*w(i);
  end;
  for i = 1:m
  y(i) = grahm_schmidt_process(z(i));
  end;
  for i = 1:m
  L(k,i) = log(norm(y(1)));
```

```
  end;
  for i = 1:m
  w(i) = y(i)/norm(y(i))
  end;
end;
for i = 1:m
lyap(i) = (1/K_1)*sum(L(:, i));
end;
```

This way of computing the Lyapunov exponents is equivalent to Definition 3.1.1 since the orthonormal basis computed each time measures the stretching and contracting of the 'axes' of the unit m-sphere (corresponds to the original orthonormal basis) to get new 'axes' of a new ellipse (corresponds to the set $\{y_i\}$).

3.1.2 Lyapunov exponents for Hénon models

Sample Result 3.1.2. Figure 3.1 shows the values of the computed values for the Lyapunov exponents for the Hénon model over the parameter values $a \in [1, 1.4]$ with parameter $b = 0.3$. The computational parameters for this plot are: the number of iteration points is $K_1 = 10^4$, the number of values of a considered is 101, and the delta value (length of interval between values of a) is $\Delta = 0.004$.

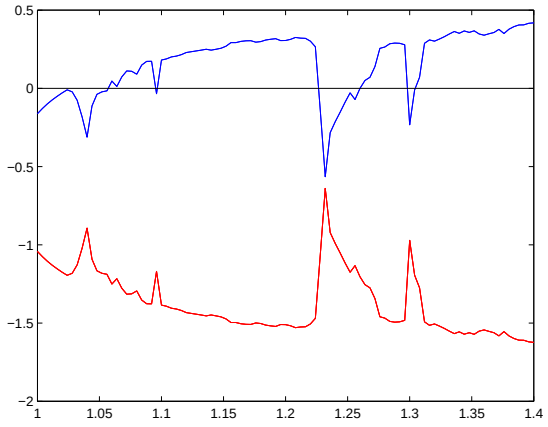

Figure 3.1: Approximate Lyapunov exponents of the Hénon model for parameters b = 0.3 and $a \in [1, 1.4]$

It will be important in Section 3.2 to have the values for all the Lyapunov exponents. However, the maximal Lyapunov exponent can indicate if a system is chaotic.

If x has a bounded orbit and the maximal Lyapunov exponent at x is positive, then the orbit of x is chaotic.

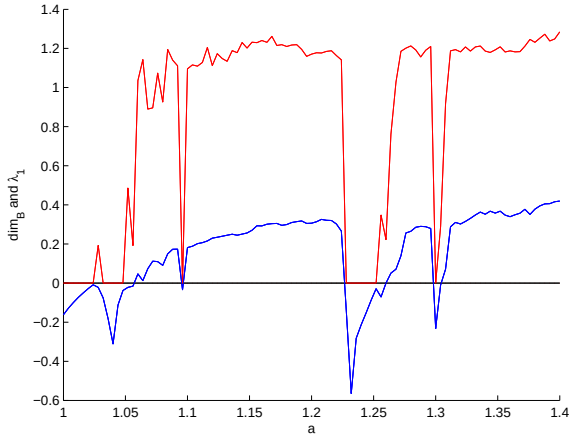

Figure 3.2: Maximal Lyapunov exponent of the Hénon model and box-counting dimension for the Hénon attractor for parameters b = 0.3 and $a \in [1, 1.4]$

Recall from Sample Result 2.5.1 that the computed approximation of box-counting dimension is sometimes positive for periodic orbits, which have box-counting dimension of zero. Figure 3.2 illustrates why this happens. An orbit converges to its forward limit set "faster" if it has a Lyapunov exponent of greater absolute value than an orbit with a Lyapunov exponent of lower absolute value. For example, at $a = 1.03$, the Lyapunov exponent gets very close to zero, which means that the orbits are converging to the attractor slower. Since we use the same number of iterations to compute dimension, we get a worse approximation in areas with a Lyapunov exponent close to zero.

Because of this property, Lyapunov exponents of a map can suggest where there may be potential numerical problems – where the maximal Lyapunov exponent is very close to zero.

3.1.3 Lyapunov exponents for LPA models

Sample Result 3.1.3. Figure 3.3 shows the computed values for all the Lyapunov exponents for the LPA model with parameter $f \in [50, 100]$, as before. Figure 3.4 shows the value of the maximal Lyapunov exponent of the LPA model. This figure suggests that there may be some problems with our numerical results for some of the parameter values $f \in [56, 68]$. In Section 3.2.2, using the Lyapunov dimension, we will show that this is the case.

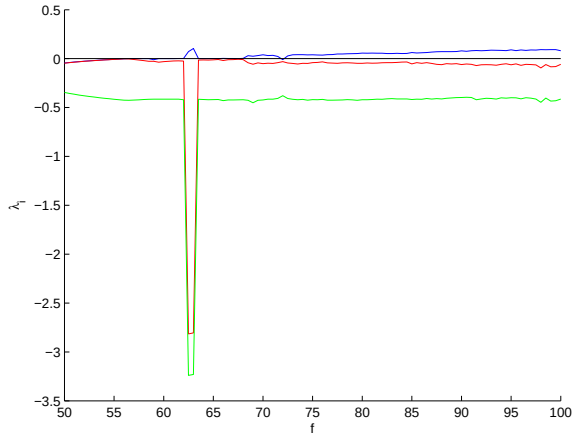

Figure 3.3: Approximate Lyapunov exponents of the LPA model for parameters

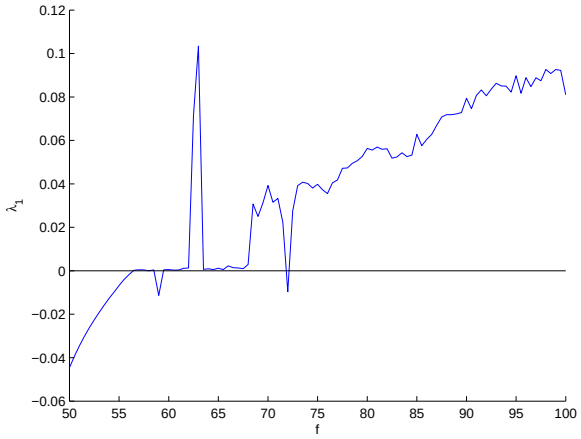

Figure 3.4: Maximal Lyapunov exponent of the LPA model for parameters

3.2 Lyapunov Dimension

The Lyapunov dimension exists for m-dimensional systems where $m \geq 2$. The Lyapunov dimension makes the measurement on the attractor based only on the Lyapunov exponents associated with the system.

Definition 3.2.1. The *Lyapunov dimension* is defined to be

$$\dim_L(S) = \begin{cases} 0 & \text{if } \lambda_1 \leq 0, \\ k + \frac{\lambda_1+\lambda_2+\ldots+\lambda_k}{|\lambda_{k+1}|} & \text{otherwise} \end{cases}$$

where λ_i is the ith greatest Lyapunov exponent ($\lambda_1 \geq \lambda_2 \geq \ldots \geq \lambda_m$), k is the largest

value such that $\sum_{i=1}^{k} \lambda_i > 0$, and S is the attractor associated with the system.

As a result of the *Kaplan-Yorke Conjecture*,

$$\dim_B \geq \dim_L,$$

so the Lyapunov dimension is a lower bound on the box-counting dimension. This means that when there is a positive Lyapunov exponent, we expect the box-counting dimension to be positive as well [10].

3.2.1 Lyapunov dimension for Hénon attractors

Sample Result 3.2.2. Figure 3.5 presents the Lyapunov dimension of the Hénon attractors over parameter $a \in [1, 1.4]$. Figure 3.6 shows the box-counting dimension and the Lyapunov dimension on the same graph. After accounting for some numerical error bounds, the box-counting dimension and Lyapunov dimension seem to agree. Where they agree, we are more certain of the accuracy of our approximation of the box-counting dimension. The few places they disagree were discussed in terms of the Lyapunov exponenets in Section 3.1.2.

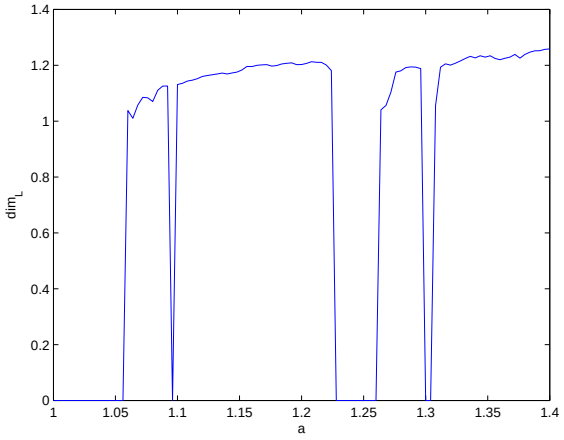

Figure 3.5: Approximate Lyapunov dimension of the Hénon attractors for parameters $b = 0.3$ and $a \in [1, 1.4]$

3.2.2 Lyapunov dimension for LPA attractors

Figure 3.7 presents the Lyapunov dimension of the LPA attractors over parameter $f \in [50, 100]$. Figure 3.8 shows the box-counting dimension and the Lyapunov dimension approximations for these models on the same graph.

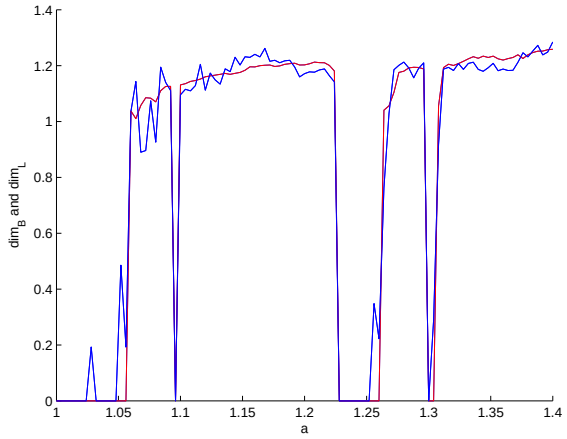

Figure 3.6: Box-counting dimension and Lyapunov dimension for Hénon attractors associated with parameters b = 0.3 and $a \in [1, 1.4]$

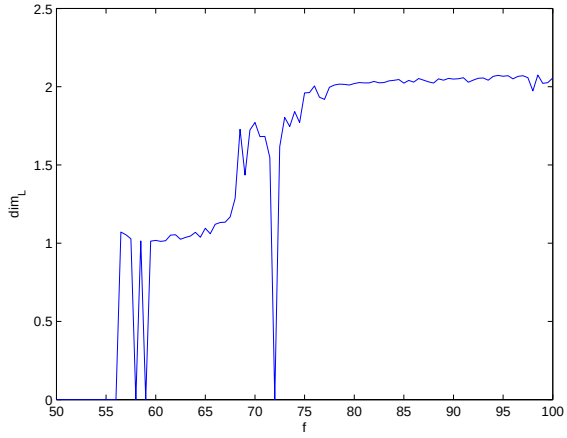

Figure 3.7: Approximate Lyapunov dimension of the LPA attractors for parameter $f \in [50, 100]$

Sample Result 3.2.3. This numerical result disagrees with what we expect to happen. We should expect the Lyapunov dimension to serve as a lower bound on the box-counting dimension of the set according to the Kaplan-Yorke Conjecture. We see the opposite result at some parameter values here.

Upon further investigation of certain problem areas, where the difference between the Lyapunov and box-counting dimension is greatest, it is likely the values for the computed Lyapunov dimension are more trustworthy and the computed values for box-counting dimension are lower than the actual values. The box-counting dimension is dependent on the ability to pick up on the fine structure of the set using ϵ-boxes.

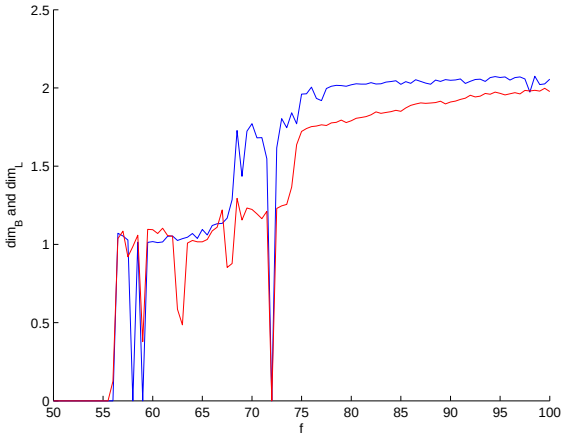

Figure 3.8: Box-counting dimension and Lyapunov dimension for LPA attractors associated with parameter$f \in [50, 100]$

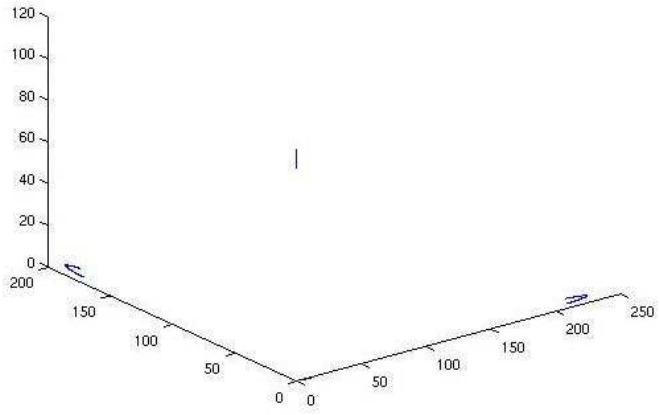

Figure 3.9: LPA attractor for parameter $f = 63$

When these boxes are not sufficiently small, the box-counting dimension may be inaccurate.

For example, for the value $f = 63$ (Figure 3.9), the computed Lyapunov dimension is greater than one, while the computed box-counting dimension is much lower. This turns out to be because the attractor bifurcates into 3 small Hénon-like attractors. Therefore, the ϵ-boxes only pick up on the period three-like behavior of the three Hénon-like attractors for an ϵ that is too large, missing the fractal structure of the small parts of the attractor.

At $f = 70.5$, in Figure 3.10, we see another large discrepancy between Lyapunov and box-counting dimensions. This is due to fine structure on the attractor that the

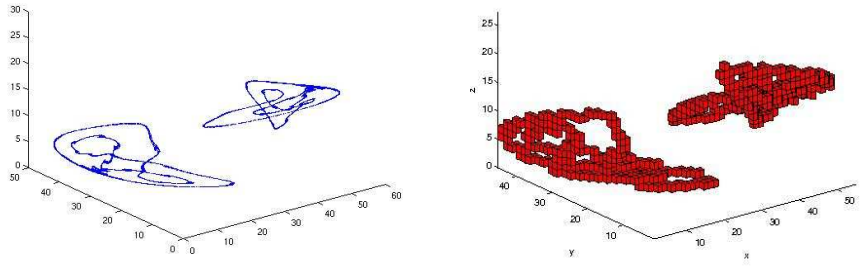

Figure 3.10: LPA attractor for parameter $f = 70.5$ and ϵ-box-covering of the attractor

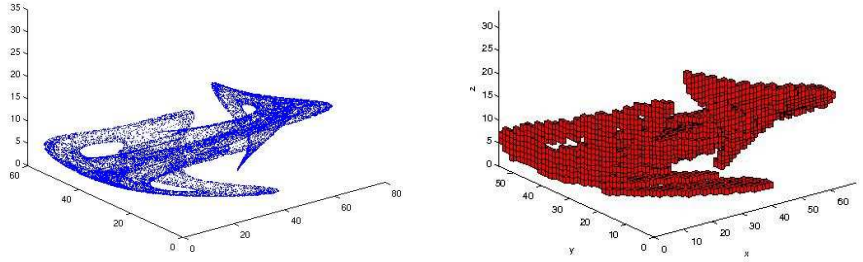

Figure 3.11: LPA attractor for parameter $f = 90$ and ϵ-box-covering of the attractor

ϵ-boxes miss, when ϵ is taken to be too large.

The true attractor seems to have a finer buzzsaw-like fractal structure that ϵ-boxes would only pick up on for very small values of ϵ. For the ϵ-boxes shown, the attractor seems closer to one-dimensional than it actually is. The same problem is likely a factor in the other areas as well, including the values obtained for parameter $f \in [75, 100]$. Though the difference is not as great in this area and numerical error may also account for differences in Lyapunov and box-counting dimensions for $f = 90$ in Figure 3.11 – the size of ϵ may be responsible for the low approximation of box-counting dimension.

Chapter 4

Infinite Dimensional Case

4.1 Box-Counting Dimension of Products of Cantor Sets

This section focuses on an analytical approach to computing the box-counting dimension of fractal-like sets defined as subsets of infinite dimensional spaces. The steps include constructing some "nice" set which should have finite box-counting dimension (here, the product of Cantor sets is used), extending the definition of the box-counting dimension to include subsets of infinite dimensional spaces, and using this definition to measure the box-counting dimension of this set. Also introduced are other techniques that may be useful when measuring the dimension of more general subsets of infinite dimensional spaces.

4.1.1 Constructing a set

Recall the following properties associated with the box-counting dimension of Cantor sets:

- We can construct a Cantor set $C \subset \mathbb{R}$ with box-counting dimension $d \in \mathbb{R}$, $0 < d < 1$. (See Theorem 2.1.6.)
- For a collection of Cantor sets $\{C_i\}$ and some finite $n \in \mathbb{N}$:

$$\dim_B(\prod_{i=1}^{n} C_i) = \sum_{i=1}^{n} \dim_B(C_i).$$

That is, the box-counting dimension of the finite Cartesian product of Cantor

sets is the sum of the box-counting dimensions of the Cantor sets. (See Theorem 2.2.3.)

We begin by constructing a set C where

$$C = \prod_{i=1}^{\infty} C_i$$

for a collection of middle 1/m Cantor sets (Section 2.1.2) such that

$$\dim_B(C_i) = \frac{1}{2^i}.$$

Since,

$$\sum_{i=1}^{\infty} \dim_B(C_i) = \sum_{i=1}^{\infty} \frac{1}{2^i} = 1,$$

we expect $\dim_B(C) = \sum_{i=1}^{\infty} \dim_B(C_i)$ as it is for finite products of Cantor sets. As we will see in Section 4.1.3, for this example, the box-counting dimension of C is 1, as expected.

4.1.2 Defining box-counting dimension for subsets of infinite dimensional spaces

Before computing the dimension of the set C, we need to extend the definition of the box-counting dimension to include subsets of the infinite dimensional space, $\mathbb{R}^\infty$, where

$$\mathbb{R}^\infty = \prod_{i=1}^{\infty} \mathbb{R}_i,\ \mathbb{R}_i = \mathbb{R}.$$

In order to extend our definition, we first need to define what an ϵ-box in $\mathbb{R}^\infty$ should be.

In finite dimensions, an ϵ-box is the product of closed intervals of length ϵ. The ϵ-boxes considered for subsets of an infinite dimensional space could naturally be defined as the infinite Cartesian product of ϵ-intervals. Consider an ϵ-box $B_B(\epsilon)$ defined as:

$$B_B(\epsilon) = \prod_{k=1}^{\infty} [c_k, c_k + \epsilon]$$

with $c_k \in \mathbb{R}$.

This definition of an ϵ-box does not work well with the definition of box-counting dimension. For many sets and $\epsilon > 0$, $N(\epsilon) = \infty$. The corresponding box-counting

dimension for these sets would be $\dim_B(S) = \infty$. This is true even when the box-counting dimension should not be infinite, for example, the set of endpoints of the unit cube, $\{0,1\}^\infty$, has box-counting dimension of infinity using this definition of an ϵ-box. This construction of a box is similar to the construction of open sets in the box-topology, which is notorious for unintuitive results.

Taking the product topology (the topology normally used for $\mathbb{R}^\infty$) into consideration, we begin by defining an ϵ-box to be the infinite product of closed sets with only a finite number of these sets given as intervals of size ϵ and the rest copies of $\mathbb{R}$. However, another parameter, n, is introduced where n is the number of these intervals of size ϵ in the product. Define an (ϵ, n)-box, $B_P(\epsilon, n)$, as:

$$B_P(\epsilon, n) = \prod_{k=1}^{n} [c_k, c_k + \epsilon] \times \prod_{k=n+1}^{\infty} \mathbb{R},$$

where $c_k \in \mathbb{R}$.

Then we may define the box-counting dimension of a set A as either Equation 4.1:

$$\dim_{B_1}(A) = \lim_{\epsilon \to 0} \lim_{n \to \infty} \frac{\ln(N(\epsilon, n))}{\ln(1/\epsilon)} \tag{4.1}$$

or Equation 4.2:

$$\dim_{B_2}(A) = \lim_{n \to \infty} \lim_{\epsilon \to 0} \frac{\ln(N(\epsilon, n))}{\ln(1/\epsilon)} \tag{4.2}$$

where $N(\epsilon, n)$ is the number of (ϵ, n)-boxes $B_P(\epsilon, n)$ needed to cover the set A, provided that the limit exists.

Using Equation 4.1, we see the same problem that occurs with the use of the definition of the ϵ-box, $B_B(\epsilon)$, giving an infinite box-counting dimension for some sets which should have finite dimension, such as $\{0,1\}^\infty$.

Equation 4.2 can be reduced to the equation:

$$\dim_{B_2}(A) = \lim_{n \to \infty} \dim_B(A_n) \tag{4.3}$$

where $\dim_B(A_n)$ is the box-counting dimension of the projection of A into the first n coordinates. However, in practice, we cannot compute the box-counting dimension directly from the definition, so instead we compute

$$\dim_B(A) = \lim_{n \to \infty} \frac{\ln(N(\epsilon_n, n))}{\ln(1/\epsilon_n)}$$

where $\epsilon_n \to 0$ as $n \to \infty$. However, the definition of box-counting dimension in Equation 4.2 is not equivalent to our practical means of computation. A counter-intuitive example is presented in Example 4.1.1.

Example 4.1.1. We start with a product of sets, all with box-counting dimension $dim_B(\hat{C}) = 0$, and show the infinite product has a positive box-counting dimension.

Recall from Section 2.1.2 the modified Cantor set, $\hat{C}$. Let

$$\hat{C_P} = \prod_{j=1}^{\infty} \hat{C_j}$$

where $\hat{C_j} = \hat{C}$ for all j.

We know that $\dim_B(\hat{C}) = 0$ from Example 2.1.8. So, what is the dimension of $\dim_B(\hat{C_P})$? Since we are taking the infinite product of this fractal, then the ϵ used to compute $\dim_B(\hat{C})$ can be used to compute $\dim_B(\hat{C_P})$ so that $\epsilon_n = 2^{-(n^2+n)}$.

So we get $N(\epsilon_n) = 2^{n^2}$, since we will have:

$N(\epsilon_1) = 2$
$N(\epsilon_2) = 4 \cdot 4$
$N(\epsilon_3) = 8 \cdot 8 \cdot 8$
$\cdots$
$N(\epsilon_n) = (2^n)^n = 2^{n^2}$
$\cdots$

Then, we can compute the dimension of $\hat{C_P}$ to be:

$$\dim_B(\hat{C_P}) = \lim_{n\to\infty} \frac{\ln(N(\epsilon_n))}{\ln(1/\epsilon_n)} = \lim_{n\to\infty} \frac{\ln(2^{n^2})}{\ln(2^{n^2+n})} = \lim_{n\to\infty} \frac{n^2}{n^2+n} = 1.$$

Even though $\hat{C}$ and any finite product of $\hat{C}$ has box-counting dimension 0, the infinite product has a positive box-counting dimension.

We borrow the idea of *regularity* from the theory of infinite dimensional systems to find a definition of box-counting dimension that behaves well. Because of regularity, attractors associated with infinite dimensional dynamical systems are subsets of a compact set S defined:

$$S = \prod_{i=1}^{\infty} S_i$$

where S_i are closed intervals $[-a_i, a_i]$ (or $[0, a_i]$), so that $\lim_{i\to\infty} i^2 \cdot a_i = 0$. For many dynamical systems, the rate at which a_i decays is exponential.

If we only consider subsets of a set S with these properties, we can define an ϵ-box, $B(\epsilon, n)$, to be:

$$B(\epsilon, n) = B_P(\epsilon, n) \cap S.$$

Then, using the definition of box-counting dimension is given by Equation 4.1 with this new $B(\epsilon, n)$:

$$\dim_B(A) = \lim_{\epsilon\to 0} \lim_{n\to\infty} \frac{\ln(N(\epsilon, n))}{\ln(1/\epsilon)}$$

will give us the definition we want. Because of the structure of S, we can reduce this definition to one with a single limit. Since $\lim_{i\to\infty} a_i = 0$, there exists some N_ϵ such that $\mu(S_i) < \epsilon$ ($\mu(S_i)$ is the length of the interval S_i) whenever $i \geq N_\epsilon$. Then

$$B_P(\epsilon, n) = B_P(\epsilon, m)$$

whenever $m, n \geq N_\epsilon$. So, we can re-define our infinite dimensional ϵ-box to be:

$$B(\epsilon) = B_P(\epsilon, N_\epsilon) \cap S.$$

Then the box-counting dimension of a set A is

$$\dim_B(A) = \lim_{\epsilon\to 0} \lim_{n\to\infty} \frac{\ln(N(\epsilon, n))}{\ln(1/\epsilon)} = \lim_{\epsilon\to 0} \frac{\ln(N(\epsilon))}{\ln(1/\epsilon)}.$$

where $N(\epsilon)$ is the number of boxes $B(\epsilon)$ needed to cover the set A. This definition looks identical to the original, finite-dimensional version of box-counting dimension.

4.1.3 Computing the dimension for our first example

Example 4.1.2. We return to our original example

$$C = \prod_{i=1}^{\infty} C_i.$$

Recall that for the sets C_i, we are removing the middle $1/m$ from all intervals starting with some initial interval for some m such that the box-counting dimension of the set C_i is equal to $1/2^i$.

Consider the subsequence $\epsilon_n = 2^{-2^n}$ and the subspace $S = \prod_{i=1}^{\infty}[0, 2^{2^i}]$. This is equivalent to considering the product of half of each C_i (since all these Cantor sets

are the union of two copies of itself). Also, to make computation easier, the length of the nth coordinate of the subspace is exactly ϵ_n. From here, we compute the number of ϵ-boxes to be

$$N(\epsilon_n) = 2^{2^i} - i - 1.$$

And from here (by L'Hopital),

$$\dim_B(C) = \lim_{n\to\infty} \frac{\ln(N(\epsilon_n))}{\ln(1/\epsilon_n)} = \lim_{n\to\infty} \frac{\ln(2^{2^n} - n - 1)}{\ln(2^{2^n})} = 1.$$

This is exactly the answer we expected.

4.2 Helpful inequalities

Several of these inequalities apply to sets in finite dimensional space, $\mathbb{R}^m$. However, these inequalities can lead to some useful results in studying infinite dimensional sets also.

For sets (such as attractors) associated with infinite dimensional models, the high, but finite, dimensional projection is often considered. Because of the "curse of dimension", where computation becomes exponentially more expensive as dimension is increased, higher dimensions create a problem for accurately computing box-counting dimension. Methods that bound the box-counting dimension are useful. Measuring the box-counting dimension of the lower-dimensional projections will not require as many iterations as the entire higher dimensional set, and we can use the values we get for these to get a bound or estimate on the box-counting dimension of the set.

4.2.1 Finite (High) Dimensional Case

Consider the standard basis $\{e_i\}$ of $\mathbb{R}^m$ where the vector $e_i \in \mathbb{R}^m$ has 1 for its ith coordinate and 0 for all other coordinates. Let $V = span\{e_j : j \in J\}$ for some set $J \subset \{1, 2, \ldots, m\}$. Then, for a point $x \in \mathbb{R}^m$ and subspace V such that $\dim(V) = span\{e_{j_1}, \ldots, e_{j_k}\}$, the *projection function* $\pi_V : \mathbb{R}^m \to \mathbb{R}^k$ projects x into subspace V:

$$\pi_V(x) = (\langle x, e_{j_1}\rangle, \ldots, \langle x, e_{j_k}\rangle) \subset \mathbb{R}^k,$$

where $\langle x, e_j\rangle$ denotes the inner product of x and e_j, which gives x_j, the projection of the point x into the jth coordinate axis. For a set $A \subset \mathbb{R}^m$,

$$\pi_V(A) = A_V = \{(\langle x, e_{j_1}\rangle, \ldots, \langle x, e_{j_k}\rangle) : x \in A\} \subset \mathbb{R}^k.$$

Two projections, A_{V_1} and A_{V_2}, are orthogonal when each vector in A_{V_1} is orthogonal to each vector in A_{V_2}. We will say that the set of n projections $\{A_{V_i} : 1 \leq i \leq n\}$ of A satisfy the *orthogonal partition property* when each vector space, V_i, is orthogonal to all other vector spaces, V_j with $j \neq i$, and $\sum_{i=1}^{n} \dim(V_i)$, that is, the orthogonal sum of all V_i is the entire space.

Then for $A \in \mathbb{R}^m$, the set of projections $\{A_{V_i}, 1 \leq i \leq n\}$ satisfy the orthogonal partition property for any set of $\{V_i = span\{e_j : j \in J_i\}\}$ where $\{J_i : 1 \leq i \leq n\}$ is a partition of $\{1, 2, \ldots, m\}$. Through some abuse of notation, for $A \subset \mathbb{R}^m$, if A_{V_i} with $V_i = span\{e_i\}$, that is, if A_{V_i} is the projection of A into the ith coordinate axis, then we let A_{V_i} be denoted A_i.

Theorem 4.2.1. *For a set, $A \subset \mathbb{R}^m$, the following inequalities hold:*

$$\frac{1}{m}\sum_{i=1}^{m} \dim_B(A_i) \leq \dim_B(A) \leq \sum_{i=1}^{m} \dim_B(A_i)$$

where A_i is the one-dimensional projection of the set into the ith coordinate axis.

Proof. First, we can show that $\dim_B(A) \leq \sum_{i=1}^{m} \dim_B(A_i)$ using Theorems 2.2.3 and 2.2.1.

We know that $A \subset \prod_{i=1}^{m} A_i$ and so

$$\dim_B(A) \leq \dim_B(\prod_{i=1}^{m} A_i) \leq \sum_{i=1}^{m} \dim_B(A_i).$$

To show $\frac{1}{m}\sum_{i=1}^{m} \dim_B(A_i) \leq \dim_B(A)$, we can show the equivalent case:

$$\sum_{i=1}^{m} \dim_B(A_i) \leq m \cdot \dim_B(A)$$

To show this, consider the definition of box-counting dimension of a set A:

$$\dim_B(A) = \lim_{\epsilon \to 0} \frac{\ln(N(\epsilon))}{\ln(1/\epsilon)}.$$

Let $N_i(\epsilon)$ be the number of ϵ-boxes needed to cover A_i. So, $N_i(\epsilon) \leq N(\epsilon)$ for all i. Then, using the definition we can show the inequality holds:

$$\begin{aligned}
\sum_{i=1}^{m} \dim_B(A_i) &= \sum_{i=1}^{m} \lim_{\epsilon \to 0} \frac{\ln(N_i(\epsilon))}{\ln(1/\epsilon)} \\
&= \lim_{\epsilon \to 0} \sum_{i=1}^{m} \frac{\ln(N_i(\epsilon))}{\ln(1/\epsilon)} \\
&= \lim_{\epsilon \to 0} \frac{\sum_{i=1}^{m} \ln(N_i(\epsilon))}{\ln(1/\epsilon)} \\
&= \lim_{\epsilon \to 0} \frac{\ln(\prod_{i=1}^{m} N_i(\epsilon))}{\ln(1/\epsilon)} \\
&\leq \lim_{\epsilon \to 0} \frac{\ln(N(\epsilon)^m)}{\ln(1/\epsilon)} \\
&= \lim_{\epsilon \to 0} \frac{m \cdot \ln(N(\epsilon))}{\ln(1/\epsilon)} \\
&= m \cdot \dim_B(A).
\end{aligned}$$

□

Theorem 4.2.1 basically says that for sets in $\mathbb{R}^m$, the box-counting dimension of one dimensional projections of the set can be used to bound the box-counting dimension of the entire set. This Theorem is just a corollary of the next theorem, Theorem 4.2.2.

Theorem 4.2.2. *For a set $A \subset \mathbb{R}^m$, let the set $\{V_i : 1 \leq i \leq n\}$ satisfy the orthogonal partition property. Then, the following inequalities hold:*

$$\frac{1}{n} \sum_{i=1}^{n} \dim_B(A_{V_i}) \leq \dim_B(A) \leq \sum_{i=1}^{n} \dim_B(A_{V_i}).$$

Proof. This proof is the same as the proof of Theorem 4.2.1, but for projections of higher dimensions. It is important that the projections are orthogonal here.

As before, $\dim_B(A) \leq \sum_{i=1}^{n} \dim_B(A_{V_i})$ using Theorems 2.2.3 and 2.2.1:

We know that $A \subset \prod_{i=1}^{n} A_{V_i}$ and so

$$\dim_B(A) \leq \dim_B(\prod_{i=1}^{n} A_{V_i}) \leq \sum_{i=1}^{n} \dim_B(A_{V_i}).$$

To show $\frac{1}{n} \sum_{i=1}^{n} \dim_B(A_{V_i}) \leq \dim_B(A)$, we can again show the equivalent case:

$$\sum_{i=1}^{n} \dim_B(A_{V_i}) \leq n \cdot \dim_B(A).$$

Let $N_i(\epsilon)$ be the number of ϵ-boxes needed to cover A_{V_i}. So, $N_i(\epsilon) \leq N(\epsilon)$ for all i. Then, using the definition we can show the inequality holds:

$$\begin{aligned}
\sum_{i=1}^{n} \dim_B(A_{V_i}) &= \sum_{i=1}^{n} \lim_{\epsilon \to 0} \frac{\ln(N_i(\epsilon))}{\ln(1/\epsilon)} \\
&= \lim_{\epsilon \to 0} \sum_{i=1}^{n} \frac{\ln(N_i(\epsilon))}{\ln(1/\epsilon)} \\
&= \lim_{\epsilon \to 0} \frac{\sum_{i=1}^{n} \ln(N_i(\epsilon))}{\ln(1/\epsilon)} \\
&= \lim_{\epsilon \to 0} \frac{\ln(\prod_{i=1}^{n} N_i(\epsilon))}{\ln(1/\epsilon)} \\
&\leq \lim_{\epsilon \to 0} \frac{\ln(N(\epsilon)^n)}{\ln(1/\epsilon)} \\
&= \lim_{\epsilon \to 0} \frac{n \cdot \ln(N(\epsilon))}{\ln(1/\epsilon)} \\
&= n \cdot \dim_B(A).
\end{aligned}$$

□

This leads to an interesting corollary:

Corollary 4.2.3. *Let the set $A \subset \mathbb{R}^m$ have projection $\pi_{V_1}(A) = A_{V_1} \subset W = \mathbb{R}^{k_1}$. Let $\pi_{V_2}(A) = A_{V_2}$ be the projection into the orthogonal complement of W. Then:*

$$\dim_B(A_{V_1}) \leq \dim_B(A) \leq \dim_B(A_{V_1}) + \dim_B(A_{V_2}).$$

Proof. This follows directly from Theorem 4.2.2.

We know $\dim_B(A_{V_1}) \leq \dim_B(A)$ since A_{V_1} is a projection of A into some subspace.

Also, $\dim_B(A) \leq \dim_B(A_1^{(k_1)}) + \dim_B(A_2^{(k_2)})$ by Theorem 4.2.2.

Corollary 4.2.3 is interesting since it may be possible to bound the box-counting dimension of a fractal lying in a very high dimensional space very closely to the box-counting dimension of lower dimensional projections. Because of the curse of dimensionality, it may be worth it to break the problem down into two smaller-dimension problem and bound the dimension of the high dimensional fractal by the dimension of its projections into lower dimension spaces. Depending on the structure of the set, it may be possible to get a very close approximation – for example, if one projection had very low or zero fractal dimension.

Theorem 4.2.4. *For a set $A \subset \mathbb{R}^m$, let the set $\{V_i : 1 \leq i \leq n\}$ satisfy the orthogonal partition property. If there are d projections such that $\dim_B(A_{V_j}) = 0$ and the number of projections of the set considered is at least 2, then:*

$$\frac{1}{n-d}\sum_{i=1}^{n}\dim_B(A_{V_i}) \leq \dim_B(A) \leq \sum_{i=1}^{n}\dim_B(A_{V_i}).$$

Proof. We know $\dim_B(A) \leq \sum_{i=1}^{n}\dim_B(A_{V_i})$ from Theorem 4.2.2.

The proof of $\frac{1}{n-d}\sum_{i=1}^{n}\dim_B(A_{V_i}) \leq \dim_B(A)$ also makes use of previous proofs. A is the subset of the product of the projections:

$$A \subset \prod_{i=1}^{n} A_{V_i} = \prod_{i=1}^{n-d} A_{V_i} \times \prod_{i=n-d+1}^{n} A_{V_i}$$

where $\dim_B(A_{V_i}) = 0$ for $i = (n-d+1), (n-d+2), \ldots, n$. This means:

$$\lim_{\epsilon \to 0} \frac{\ln(N_i(\epsilon))}{\ln(1/\epsilon)} = 0$$

for all $i = (n-d+1), (n-d+2), \ldots, n$.

Now, let $N_i(\epsilon)$ be the number of ϵ-boxes needed to cover A_{V_i}. As before, $N_i(\epsilon) \leq N(\epsilon)$ for all i. Then, using the definition we can show the inequality holds:

$$\begin{aligned}
\sum_{i=1}^{n}\dim_B(A_i^{(1)}) &= \sum_{i=1}^{n-d}\dim_B(A_i^{(1)}) + \sum_{i=n-d}^{n}\dim_B(A_i^{(1)}) \\
&= \sum_{i=1}^{n-d}\dim_B(A_i^{(1)}) + \sum_{i=n-d}^{n} 0 \\
&= \sum_{i=1}^{n-d}\dim_B(A_i^{(1)}) + 0 \\
&= \sum_{i=1}^{n-d}\dim_B(A_i^{(1)}) \\
&\leq (n-d)\cdot\dim_B(A).
\end{aligned}$$

The last inequality holds by Theorem 4.2.2. So $\sum_{i=1}^{n}\dim_B(A_i^{(1)}) \leq (n-d)\cdot\dim_B(A)$. Dividing both sides by $n-d$ gives the inequality we want. □

4.2.2 Extension to infinite dimensional case

This theorem results from extending the ideas from the previous section to infinite dimensional spaces. This theorem will be useful in the next chapter when measuring the box-counting dimension of the infinite dimensional Kot-Schaffer attractor.

Theorem 4.2.5. *For $A \subset \mathbb{R}^\infty$, suppose the set $\{V_i : i \geq 1\}$ satisfies the orthogonal partition property (where all projections are orthogonal and the orthogonal sum of the phase spaces of each projection gives all of $\mathbb{R}^\infty$). If $\dim_B(\prod_{i=N+1}^{\infty}(A_{V_i})) = 0$ for some N (for example, if this product were a single point), then*

$$\frac{1}{N}\sum_{i=1}^{N}\dim_B(A_{V_i}) \leq \dim_B(A) \leq \sum_{i=1}^{N}\dim_B(A_{V_i}).$$

Proof. If we consider $A^{(N)} = \pi^{(N)}(A) \subset \mathbb{R}^N$, the projection of A into the first N coordinates, then

$$\frac{1}{N}\sum_{i=1}^{N}\dim_B(A_{V_i}) \leq \dim_B(A^{(N)}) \leq \sum_{i=1}^{N}\dim_B(A_{V_i})$$

by Theorem 4.2.2. Then,

$$\dim_B(A^{(N)}) \leq \dim_B(A)$$

since the dimension of a projection is less than the dimension of the whole set. Also,

$$\dim_B(A) = \dim_B\left(A^{(N)} \times \prod_{i=N+1}^{\infty} A_{V_i}\right) \leq \dim_B(A^{(N)}) + \dim_B\left(\prod_{i=N+1}^{\infty} A_{V_i}\right) = \dim_B(A^{(N)}) + 0 = \dim_B$$

So, $\dim_B(A) \geq \dim_B(A^{(N)})$ and $\dim_B(A^{(N)}) \leq \dim_B(A)$. But then $\dim_B(A^{(N)}) = \dim_B(A)$. Substituting $\dim_B(A)$ for $\dim_B(A^{(N)})$, we get:

$$\frac{1}{N}\sum_{i=1}^{N}\dim_B(A_{V_i}) \leq \dim_B(A) \leq \sum_{i=1}^{N}\dim_B(A_{V_i}).$$

□

Chapter 5

Kot-Schaffer Example

5.1 Infinite Dimensional Dynamical Systems

Recall that the box-counting dimension of a chaotic attractor is measured computationally because of the difficulty in describing an attractor analytically. Another complication is added to the problem when considering attractors associated with infinite dimensional systems that are subsets of an infinite dimensional phase space. In this chapter, a specific example of such a chaotic attractor associated with the Kot-Schaffer Model is considered. The properties associated with this model that allows one to understand and make computations on the attractor and dynamics of the system hold for a whole class of other infinite dimensional dynamical systems as well.

5.2 Kot-Schaffer Model

Recall from Section 1.2.3 that the Kot-Schaffer map $\Phi : L^2([-\pi, \pi]) \to L^2([-\pi, \pi])$ is defined for $a \in: L^2([-\pi, \pi])$:

$$\Phi[a](y) := \frac{1}{2\pi} \int_{-\pi}^{\pi} b(x, y) g[a](x) dx, \tag{5.1}$$

where the dispersal kernel b has the property that $b(x, y) = b(x - y) \in L^2([-\pi, \pi])$ and the logistic growth operator g is defined:

$$g[a](x) := \mu a(x) \left(1 - \frac{a(x)}{c(x)}\right)$$

with $\mu > 0$ and $c \in L^2([-\pi, \pi])$.

We expand b, c, and a using the Fourier modes, an orthonormal basis for L^2, $\{\varphi_k(x) = e^{ikx} : k \in \mathbb{Z}\}$, so that $b(x, y) = b(x-y) = \sum_{k=0}^{\infty} b_k \varphi(x-y)$ where $b_k = 2^{-|k|}$, $a = \sum_k a_k \varphi_k$, and $c = \sum_k c_k \varphi_k$. Let $a_k, b_k, c_k \in \mathbb{C}$ be the coefficients of the Fourier expansions of a,b, and c^{-1}, respectively, with $a_k = a_{-k}$, $b_k = b_{-k}$, and $c_k = c_{-k}$ for all $k \in \mathbb{Z}$. Then, rewriting Equation (5.1) using these Fourier mode expansions results in the decomposition of $\Phi[a]$ into a countable set of maps on the Fourier coefficients of a:

$$f_k : a_k \mapsto \mu b_k \left[a_k - \sum_{j+l+n=k} c_j a_l a_n \right], k \in \mathbb{Z} \tag{5.2}$$

where we recall $a_k = a_{-k}$, $b_k = b_{-k}$, and $c_k = c_{-k}$ for all $k \in \mathbb{Z}$.

From here, we take the *Galerkin projection* of the countable map to obtain a finite dimensional system of maps. The original system is truncated so that only the first m modes are considered, while all Fourier coefficients a_k with $k \geq m$ are set to equal zero. The m-dimensional projection of the Kot-Schaffer map is the map $f^{(m)} : \mathbb{R}^m \to \mathbb{R}^m$ defined for $k = 0, 1, \ldots, m-1$:

$$f_k^{(m)} : a_k \mapsto \mu b_k \left[a_k - \sum_{\substack{j+l+n=k \\ 0 \leq |l|, |n| \leq m-1}} c_{|j|} a_{|l|} a_{|n|} \right], \tag{5.3}$$

with parameters $\mu, b_k, c_{|j|} \in \mathbb{R}$ [4].

This process of decomposing an infinite dimensional dynamical system into Fourier modes to obtain a countable system of maps and then performing a Galerkin projection into the first m modes can generally be used to obtain a finite dimensional dynamical system. Because of a property common to most infinite dimensional dynamical systems called *regularity*, this finite dimensional dynamical system retains the 'essential information' about the original dynamical system. When considering a decomposition into Fourier modes, regularity refers to the rate at which the Fourier modes $a_k \to 0$ as $k \to \infty$. (See Equation (5.4)). More specifically, upon one iteration of the map, a point in the countable dimensional space is taken inside a compact subspace of the infinite dimensional space where there is exponential decay in the higher modes. Because of this property, any attractor associated with the countable system of maps will lie inside of this compact subset of $\mathbb{R}^\infty$. For the Kot-Schaffer

model, this is demonstrated by the following result:

$$\langle \Phi(a), \varphi_k \rangle \leq ||g[a]|| b_k \tag{5.4}$$

where $||g[a]||$ depends only on the form of g and the input $a \in L^2([-\pi, \pi])$ and does not depend on k. Since $b_k = 2^{-k}$ and $||g[a]||$ is constant, there is strong decay toward zero in the higher modes of a [3].

There are typically a finite number of coordinates, called the *determining modes*, which are sufficient to obtaining the important information about the original system. In practice, the number of determining modes is determined through simulations and numerical experiments. In [3], techniques based on algebraic topology indicate that the first five modes of the Kot-Schaffer map should contain the determining modes.

5.3 The Box-counting Dimension of the Kot-Schaffer Attractor

Since the attractor associated with the countable system of maps must lie within a compact subspace of $\mathbb{R}^\infty$, we can apply the definition of box-counting dimension extended to infinite dimensional spaces. Since there is significant exponential decay in the higher modes of the Fourier expansion, we assume the box-counting dimensions of the projection of the map in these coordinate directions are all equal to zero. Then we may apply Theorem 4.2.5 and only consider the box-counting dimension of the finite-dimensional projection of the set into the determining modes.

This is a huge assumption about the system. It assumes that we can ignore all the fractal structure present in the higher modes. However, from a computational point of view, because of the strong decay in the higher modes, the fractal structures in these modes are ignored since they "look like" fixed points to the computer (at some fixed ϵ value). There is some numerical justification for this assumption presented in this section. The determining modes, which supposedly hold the important dynamical information associated with the system is a good starting point when considering finite dimension projections.

Sample Result 5.3.1. We let $K_1 = 10^6$.

Recall that the depth$= m \cdot s$ where m is the dimension of the phase space and s corresponds the number of times the initial box size ϵ_0 has been halved.

For a depth of 15, we get an approximation for box-counting dimension $\dim_B \approx$

1.73. For a depth of 20, we get an approximation for box-counting dimension $\dim_B \approx$ 1.77. For a depth of 25, we get an approximation for box-counting dimension $\dim_B \approx$ 1.74.

So, our approximation for box-counting dimension seems to lie between 1.7 and 1.8.

5.3.1 Related measurements of box-counting dimension

This first result measures the box-counting dimension as phase space dimension m increases to $m = 10$.

Sample Result 5.3.2. Consider the finite projection of the Kot-Schaffer model onto the first 10 modes. So, the dimension of the phase space is 10. We let $K_1 = 10^6$.

For a depth of 20, we get an approximation for box-counting dimension $\dim_B \approx$ 1.88. For a depth of 30, we get an approximation for box-counting dimension $\dim_B \approx$ 1.67. For a depth of 40, we get an approximation for box-counting dimension $\dim_B \approx$ 1.65.

For these higher values of depth, there is likely a problem with our approximation related to our iteration number K_1. Although the zeroth Betti number associated with this map at these depths indicates the box-covering is still a connected set, it is still possible that some boxes in the 'true' box covering have been missed.

That being said, it does appear that the box-counting dimension of the set lying in the 10-dimensional space has a box-counting dimension close to the dimension of the set lying in the 5-dimensional space. Theoretically, it would have been possible for these dimensions to be much higher (+5 dimensional).

The next result also shows that the box-counting dimension does not vary too much as projections are taken:

Sample Result 5.3.3. Here, we consider the 5-dimension Kot-Schaffer model with $K_1 = 10^6$. We consider the dimensions of the projection of the Kot-Schaffer attractor into the first 2, first 3, and first 4 modes at a depth of 25:

The approximate box-counting dimension for the projection of the attractor onto the first 2 modes is $\dim_B \approx 1.67$. The approximate box-counting dimension for the projection of the attractor onto the first 3 modes is $\dim_B \approx 1.70$. The approximate box-counting dimension for the projection of the attractor onto the first 4 modes is $\dim_B \approx 1.72$.

Recall that the approximate box-counting dimension for the attractor associated with the 5-dimensional model at this depth is $\dim_B = 1.74$. It appears that the

dimension does not increase much as we increase the projection dimension. This seems to further convince us that we may be able to approximate the box-counting dimension of the entire infinite-dimensional attractor by the m-dimensional projections of the attractor.

5.4 The Lyapunov Dimension of the Kot-Schaffer Attractor

In order to compute the Lyapunov dimension of the attractor associated with our set of maps, we first must determine the derivative (or Jacobian) associated with the set of maps to determine the Lyapunov exponents. From here, we may compute the Lyapunov dimension to estimate the accuracy of our measurement of the box-counting dimension of the attractor.

5.4.1 Derivative of the Kot-Schaffer Model

In order to compute the Lyapunov exponents associated with the Kot-Schaffer model, we first need to compute the Jacobian associated with the system of maps. Recall Equation (5.2):

$$f_k : a_k \mapsto \mu b_k \left[a_k - \sum_{j+l+n=k} c_j a_l a_n \right]. \tag{5.5}$$

is the decomposition of the Kot-Schaffer model into Fourier modes.

Then the partial derivative of the function f_k with respect to the mode a_i for

$k, i \in \mathbb{Z}$ is:

$$\begin{aligned}
\frac{\partial f_k}{\partial a_i} &= \mu b_k \left[\delta_{ki} - \frac{\partial}{\partial a_i} \sum_{j+l+n=k} c_j a_l a_n \right] \\
&= \mu b_k \left[\delta_{ki} - \frac{\partial}{\partial a_i} \left(\sum_{\substack{j+l+n=k \\ n=\pm i, l \neq \pm i}} c_j a_l a_n + \sum_{\substack{j+l+n=k \\ n \neq \pm i, l=\pm i}} c_j a_l a_n + \sum_{\substack{j+l+n=k \\ n=\pm i, l=\pm i}} c_j a_l a_n \right) \right] \\
&= \mu b_k \left[\delta_{ki} - \sum_{\substack{j+l+n=k \\ n=\pm i, l \neq \pm i}} c_j a_l - \sum_{\substack{j+l+n=k \\ n \neq \pm i, l=\pm i}} c_j a_n - 2 \cdot \sum_{\substack{j+l+n=k \\ n=\pm i, l=\pm i}} c_j a_l \right] \\
&= \mu b_k \left[\delta_{ki} - 2 \cdot \sum_{\substack{j+l+n=k \\ n=\pm i, l \neq \pm i}} c_j a_l - 2 \cdot \sum_{\substack{j+l+n=k \\ n=\pm i, l=\pm i}} c_j a_l \right] \\
&= \mu b_k \left[\delta_{ki} - 2 \cdot \sum_{\substack{j+l+n=k \\ n=\pm i}} c_j a_l \right] \\
&= \mu b_k \left[\delta_{ki} - 2 \cdot \sum_{j+l=k \pm i} c_j a_l \right]
\end{aligned}$$

where $a_k = a_{-k}, c_k = c_{-k}$.

We define the Jacobian of the matrix entry-wise as:

$$J = [J]_{k,i} = \left[\frac{\partial f_k}{\partial a_i} \right]_{k,i} = \begin{bmatrix} \frac{\partial f_0}{\partial a_0} & \frac{\partial f_0}{\partial a_1} & \cdots \\ \frac{\partial f_1}{\partial a_0} & \ddots & \\ \vdots & & \end{bmatrix}. \tag{5.6}$$

Then, the Jacobian associated with the m-dimensional Galerkin projection of the model (Equation (5.3)) is the $m \times m$ matrix: $J = [J]_{k,i} = \left[\frac{\partial f_k}{\partial a_i} \right]_{k,i}$ for $k, i = 0, 1, \ldots m-1$ where the partial derivatives are:

$$\frac{\partial f_k}{\partial a_i} = \mu b_k \left[\delta_{ki} - 2 \cdot \sum_{j+l=k \pm i} c_j a_l \right] \tag{5.7}$$

where $a_k = 0$ whenever $k \geq m$.

Computationally, we have the following algorithm:

```
D = eye(m)     % D is the identity of size m x m.
x(1:m) = x_0, elsewhere we define it as zero

for k = 0:m-1
  for i = 0:dim-1
    for j = -J:J
      if i == 0
        D(k,i) = D(k,i) - 2*c(abs(j))*x(abs(k-j));
      else
        D(k,i) = D(k,i) - 2*c(abs(j))*x(abs(k-i-j)) - 2*c(abs(j))*x(abs(k+i-j));
      end;
    end;
  end;
  D(k,:) = mu*b(k)*D(k,:);
end;

Then D is the Jacobian.
```

5.4.2 Lyapunov exponents for the Kot-Schaffer model

This result is the approximation of the Lyapunov expoenents associated with

Sample Result 5.4.1. Let the number of iterations considered be $K_1 = 10^5$. Then the Lyapunov exponents of the system are computed to be:
$\lambda_1 = 0.344$
$\lambda_2 = -0.323$
$\lambda_3 = -1.318$
$\lambda_4 = -1.972$
$\lambda_5 = -2.763$
The positive maximal Lyapunov exponent suggests that, as suspected, the system does exhibit chaos.

5.4.3 Lyapunov dimension of the Kot-Schaffer attractor

Sample Result 5.4.2. Using the values of the Lyapunov exponents from Sample Result 5.4.1, the Lyapunov dimension of the Kot-Schaffer attractor is approximated to be 2.017.

5.5 Interpretation of the Results

So we have two approximations for the box-counting dimension from the two different methods – direct computation and computation of the lower bound Lyapunov dimension. The box-counting dimension of the attractor for the 5-dimensional projection of the Kot-Schaffer model was approximated to lie between 1.7 and 1.8. The Lyapunov dimension suggests that the true box-counting dimension of this attractor should be at least 2.017.

The Lyapunov exponents from the Sample Result 5.4.1 suggest there is potential for error since $\lambda_1 + \lambda_2$ is very close to zero. However, if $\lambda_1 + \lambda_2$ were negative instead of positive (as it is assumed to be for these values), then the Lyapunov dimension would be very close to one, which does not seem to be the case based on numerical evidence (the dimension of a 2-dimensional projection has box-counting dimension much greater than 1 (at least 1.6). So we conclude that our approximation of the Lyapunov dimension is relatively trustworthy. This means that our approximation for the box-counting dimension of the attractor is low.

The reason for this discrepancy could result from too few iteration points, but it is also possible that our ϵ-boxes were too large to pick up on some of the finer structure in the attractor, similar to the buzz-saw attractor in Section 3.2.2.

Chapter 6

Conclusion

This paper focused on aspects of the definition of box-counting dimension, one measure of the chaos associated with a dynamical system. For subsets of finite dimensional spaces, we computed the box-counting dimension of several examples and discussed properties, both analytical and computational, associated with box-counting dimension. In order to estimate the accuracy of the computational approximation of the box-counting dimension of a set, we introduce a related measurement on chaos, the Lyapunov dimension. Following this, we extended the definition of box-counting dimension to include subsets of infinite dimensional spaces. Then, finally, we used this definition, properties of infinite dimensional dynamical systems, and our knowledge of box-counting dimension in the finite dimensional spaces to compute an approximation for the box-counting dimension of the attractor associated with the infinite-dimensional Kot-Schaffer Model.

It is possible for the work presented in this paper to be extended further. It may be interesting to explore other methods of bounding or better approximating box-counting dimension of an attractor lying in a high-dimensional phase space with a relatively low computational cost. One option may be to attempt to use the inequalities from Chapter 4 to find a relatively tight bound on the box-counting dimension. In order to do this however, it might be better (in order to get tighter bounds) to consider a different orthonormal basis of R^m and consider projections onto spans of sets of these vectors (satisfying the orthonormal partition property). Another possible direction could be to define a more computational-based definition of box-counting dimension, one that only considered grids up to some fixed ϵ. If one assumes self-similarity in a set, then this idea should yield interesting and meaningful results. Basically, there is still a lot of research that can be done on topics related to those of this paper.

Bibliography

[1] CHomP (Computational Homology Project). http://chomp.rutgers.edu.

[2] Kathleen Alligood, Tim Sauer, and James Yorke. *Chaos: An Introduction to Dynamical Systems*. Springer Science+Business Media, LLC, New York, 1996.

[3] Sarah Day. Towards a rigorous numerical study of the kot-schaffer model. *Dynamic Systems and Applications*, 11:87–97, 2002.

[4] Sarah Day. *A Rigorous Numerical Method in Infinite Dimensions*. PhD thesis, Georgia Institute of Technology, 2003.

[5] Sarah Day, Konstantin Mischaikow, and Oliver Junge. A rigorous numerical method for the global analysis of infinite-dimensional discrete dynamical systems. *SIAM Journal on Applied Dynamical Systems*, 3:117–160, 2004.

[6] Kenneth Falconer. *Techniques in Fractal Geometry*. John Wiley & Sons Ltd., West Sussex, 1997.

[7] Kenneth Falconer. *Fractal Geometry: Mathematical Foundations and Applications*. John Wiley & Sons Ltd., West Sussex, 2nd edition, 2003.

[8] Tomasz Kacynski, Konstantin Mischaikow, and Marian Mrozek. *Computational Homology*. Springer, New York, 2004.

[9] G. Froyland M. Dellnitz and O. Junge. GAIO (Global Analysis of Invariant Objects). http://mathwww.uni-paderborn.de/ agdellnitz/gaio/.

[10] Heinz-Otto Peitgen, Hartmut Jrgens, and Dietmar Saupe. *Chaos and Fractals: New Frontiers of Science*. Springer, 2004.

[11] Stefan Siegmund and Peter Taraba. Approximation of box dimension of attractors using the subdivision algorithm. *Dynamical Systems*, 21:1–24, 2006.

[12] Ilie Ugarcovici and Howard Weiss. Chaotic dynamics of a nonlinear density dependent population model. *Nonlinearity*, 17:1689–1711, 2004.